QUICK LOOK REPORT ON

SEMISCALE MOD-1 TESTS S-28-1 AND S-28-2

STEAM GENERATOR TUBE RUPTURE TESTS

SEMISCALE PROGRAM

July 1977

Prepared for the

U. S. Nuclear Regulatory Commission

EG&G Idaho, Inc.

IDAHO NATIONAL ENGINEERING LABORATORY

ENERGY RESEARCH AND DEVELOPMENT ADMINISTRATION

IDAHO OPERATIONS OFFICE UNDER CONTRACT EY-76-C-07-1570

PRELIMINARY

QUICK LOOK REPORT ON

SEMISCALE MOD-1 TESTS S-28-1 AND S-28-2

STEAM GENERATOR TUBE RUPTURE TESTS

by

J. M. Cozzuol

SEMISCALE PROGRAM

Approved: _____

D. J. Olson, Manager
Semiscale Program

Approved: _____

D. J. Hanson
Semiscale Experiment Specification & Analysis Branch

The information contained in this summary report is preliminary and incomplete. Selected pertinent data are presented in order to draw preliminary conclusions and to expedite the reporting of research results.

PRELIMINARY

List of Figures

List of Figures (Contd)

List of Figures (Contd)

Summary

This report presents a preliminary evaluation of the results from Semiscale Mod-1 Tests S-28-1 and S-28-2. These integral blowdown-reflood tests were conducted with a break configuration representative of a 200% double-ended offset shear cold leg break, and included the simulation of steam generator tube ruptures at the initiation of refill. The purpose of these tests was to evaluate the effect of the steam generator secondary-to-primary flow on the overall system hydraulic response and on the core thermal response. The primary objective of Test S-28-1 was to determine the effect of a relatively large steam generator secondary-to-primary flow on the core thermal response, and in so doing, to establish a basis for determining an upper limit on the range of steam generator tube ruptures which could lead to high rod cladding temperatures. The primary objective of Test S-28-2 was to determine the effect of a small secondary-to-primary flow on the core thermal behavior and thus to establish a basis for determining a lower limit on the range of steam generator tube ruptures which could lead to high rod cladding temperatures.

The test conditions for Tests S-28-1 and S-28-2 were essentially the same as those of the Series 28 baseline test (Test S-04-6), except for the introduction of the secondary-to-primary mass flow to simulate the steam generator tube ruptures. The tube rupture flow was simulated by a controlled injection from a heated accumulator tank into the intact loop hot leg between the steam generator inlet plenum and the pressurizer. The steam generator secondary-to-primary flow for Test S-28-1 simulated the flow from the single-ended rupture of a total of 60 tubes in 3 of 4 steam generators in a 4 loop PWR. The secondary-to-primary flow for Test S-28-2 simulated the flow from the rupture of a total of only 6 tubes in 3 of 4 steam generators in a 4 loop PWR. The steam generator tube rupture flow was begun at the initiation of refill (at about 40 seconds after rupture) for both tests. The water in the heated accumulator tank was maintained at about 547°K (approximately the average temperature of the PWR steam generator secondary fluid at rated load) and 7584 kPa. During the period of tube rupture flow, the heat transfer potential of the intact loop steam generator was simulated by discharging (to atmosphere) the steam generator secondary fluid at a rate equivalent to the tube rupture injection rate.

During the period of simulated generator flow for Test S-28-1, the secondary-to-primary flow was the dominant influence on the overall system and core hydraulic response. The steam generator injection resulted in a strong reverse core flow during most of the injection period. The strong reverse core flow physically delayed the initiation of vessel refill until about 110 seconds (as compared to about 40 seconds for the baseline Test S-04-6) and also delayed the refill of the lower plenum until after the steam generator liquid inventory was depleted at about 242 seconds after rupture. The initiation of reflood was then accomplished by the intact loop low pressure injection system (LPIS) and occurred at about 255 seconds.

PRELIMINARY

The core thermal response for Test S-28-1 was characterized by a rapid top-down quench of the entire core following the initiation of the steam generator secondary-to-primary flow. The rapid cooling and resulting early quenching of the core are attributed to fairly low quality fluid entering the top of the vessel from the steam generator secondary. Once quenching occurred, the rod cladding temperatures remained near the system saturation temperature until the steam generator injection ceased. Following the cessation of the secondary-to-primary injection, a period of core heatup occurred, but the LPIS flow was sufficient to cause requenching by about 300 seconds. The maximum cladding temperatures during this heatup period did not exceed 620°K. As a result of the excellent core cooling following the initiation of the secondary-to-primary injection, the maximum cladding temperatures during the period of the injection occurred at the initiation of the secondary-to-primary flow, and were considerably lower than the maximum cladding temperatures during the blowdown period.

Unlike Test S-28-1, the secondary-to-primary injection rate for the test simulating a small number of ruptured tubes (Test S-28-2) was not of sufficient magnitude to maintain a reverse core flow for the entire tube rupture flow period. The steam generator tube rupture injection caused the core flow to remain negative until the initiation of the intact loop accumulator nitrogen injection. The initiation of nitrogen injection at about 66 seconds forced the initiation of vessel refill and resulted in reflood beginning at about 80 seconds (as compared to about 58 seconds for the baseline Test S-04-6). The secondary-to-primary injection during the reflood period did not appear to significantly affect the rate of reflood.

The core thermal response following 40 seconds for Test S-28-2, although similar to the response for Test S-04-6, was influenced considerably by the steam generator secondary-to-primary injection. However, the peak cladding temperatures for the two tests were essentially the same. A core maximum temperature of 1092°K was observed for Test S-28-2 while the maximum temperature for Test S-04-6 was about 1075°K. The effect of the tube rupture injection was to delay, somewhat, the quench times, especially in the lower and upper portions of the core. In addition, the peak cladding temperatures occurred considerably later in the reflood phase of the test than occurred for Test S-04-6. In Test S-04-6 most of the peak cladding temperatures occurred shortly following the initiation of reflood, whereas for Test S-28-2 the peak cladding temperatures occurred after 100 seconds.

Introduction

As part of the overall Semiscale blowdown and emergency core cooling project conducted by EG&G Idaho, Inc., the Semiscale Mod-1 experimental program is used to investigate the thermal and hydraulic phenomena accompanying a hypothesized loss-of-coolant accident (LOCA) in a water-cooled nuclear reactor system. The general objective of the Semiscale

Program is to obtain representative integral and separate effects thermal-hydraulic response data to provide an experimental basis for analytical model development and verification.

The purpose of Test Series 28 (designated the steam generator tube rupture test series) is to investigate the influence of the rupture of steam generator tubes on the core and system response during a hypothetical large break loss-of-coolant accident (LOCA). Data from Test Series 28 will be used to determine the sensitivity of core peak cladding temperatures to the magnitude of the flow rate from the secondary side of the steam generator to the primary system. The data will also be used to evaluate the capability of current models to predict the thermal-hydraulic phenomena that are expected to occur during the refill and reflood phases of a LOCA with steam generator tube ruptures.

This document contains a preliminary analysis of the results obtained from the first and second tests (designated Tests S-28-1 and S-28-2) of the steam generator tube rupture test series conducted in the Semiscale Mod-1 system. Tests S-28-1 and S-28-2 were both conducted with a break configuration representative of a 200% double-ended offset shear cold leg break. The secondary-to-primary flow due to the rupture of steam generator tubes was simulated by injection of fluid at a temperature typical of a PWR steam generator secondary into the intact loop hot leg between the steam generator inlet plenum and the pressurizer. The injection was accomplished using a pressurized water source. For Test S-28-1 fluid was injected at a rate of approximately 0.54 kg/s to simulate flow from the single-ended rupture of 60 tubes[a] in a PWR steam generator, while for Test S-28-2 fluid was injected at a rate of 0.054 kg/s to simulate the flow from 6 tubes in a PWR steam generator. The steam generator tube rupture flow for both tests was begun at about 40 seconds[b] after the initiation of the cold leg break, and continued until about 242 seconds for Test S-28-1 and for the duration of the test (640 seconds)

---

[a] To provide a basis for comparing the relative magnitudes of the tube rupture mass flow rates in the Semiscale Mod-1 system and a PWR, the magnitudes of the steam generator secondary-to-primary mass flow rates in the Mod-1 system are presented in terms of the flow rates associated with a given number of single-ended tube ruptures in a PWR steam generator.

[b] 40 seconds is approximately the time at which vessel refill would have begun if the steam generator tube rupture injection had not occurred. Analysis indicates that a steam generator tube rupture at the initiation of refill would result in a more sever core thermal response than would occur if the steam generator tubes ruptured either during blowdown or later during reflood.

for Test S-28-2. The change in heat transfer potential of the steam generator was simulated by discharging the steam generator secondary fluid at a rate equivalent to the rate of the tube rupture flow. The system initial conditions and emergency core coolant (ECC) injection parameters for Tests S-28-1 and S-28-2 were essentially the same as the baseline test for Series 28, Test S-04-6 (Reference 1).

To assist in understanding the data presented in this report, Figure 1 provides and isometric view of the Mod-1 system together with the general location of the instrumentation. The Semiscale Mod-1 system configuration and the instrumentation for Test Series 28 are described in Reference 2.

The powered heater rod configuration for Tests S-28-1 and S-28-2 was identical to that for Test S-04-6. Figure 2 shows the core heater rod arrangement and includes the locations of unpowered and high-powered heater rods. Thirty-six of the 40 heater rods were powered in each test. Four rods (rods C3, F3, D5 and F6) were unpowered to make the core bundle more representative of a PWR fuel assembly containing control rod thimbles and instrument tubes. The three center rods (rods D4, E4, and E5) were operated at a 5% higher peak power density than the remaining 33 powered rods to simulate the radial power profile near a control rod thimble in a PWR fuel assembly.

Figure 3 shows the Mod-1 heater rod normalized axial power profile. The low power heater rods had a peak power density of about 37.7 kW/m, whereas the three center rods had a peak power density of about 39.7 kW/m. The initial portion of the core power decay curves for Tests S-28-1 and S-28-2 are shown in Figures 4 and 5 respectively. For comparison purposes, the core power decay curve for Test S-04-6 is included in the figures.

The specified initial conditions and operational variables together with the actual test conditions for Tests S-28-1 and S-28-2 are listed in Tables I and II respectively. Initial prerupture conditions for each test were compared with the specified prerupture conditions and the differences were judged to be minor. These minor differences in conditions prior to rupture for Tests S-28-1 and S-28-2 did not significantly influence the postrupture system behavior.

Pretest predictions of the thermal-hydraulic response for Test S-28-1 (Reference 3) and Test S-28-2 (Reference 4) were obtained using Test S-04-6 data and the FLOOD4 computer code. The system response during the first 40 seconds of Tests S-28-1 and S-28-2 was expected to be the same as the system response in Test S-04-6. Therefore, Test S-04-6 data was used to provide the initial conditions for the FLOOD4 calculations starting at 40 seconds after rupture. The FLOOD4 code was then used to provide the

TABLE I

TEST AND PRERUPTURE CONDITIONS FOR TEST S-28-1

Primary System	Specified Condition	Test Condition
Core Power (AMPCOR-T) (VOLTCOR-T) (MW)	1.44	1.44
System pressure (PV+10) (kPa, gage)	15513 ± 172	15706
Loop temperature		
Intact loop cold leg (RBU-14 (°K)	557.8 ± 1	558
Intact loop hot leg (RBU-2) (°K)	594.4 ± 1	594
Broken loop hot leg (TFB-30) (°K)	591.7 ± 3	591
Core flow rate (FTV-COREIN) L^3/min	562 ± 18	556
Pressure suppression system		
Tank water temperature (TF-PSS-33) (°K)	Ambient	288
Tank water pressure (P-PSS) (kPa, gage)	155 ± 7	145
Pressurizer water (DPU-PRESLL) (kg)	9.07	9.5
Steam generator feedwater temperature (TFU-SGFW) (°K)	497 ± 6	480
Steam generator secondary liquid level (DPU-SG-SEC) (cm)	295 ± 5	286

TABLE I (contd)

TEST AND PRERUPTURE CONDITIONS FOR TEST S-28-1

ECC System	Specified Condition	Test Condition
Accumulator CI-T-1 (Unbroken loop)		
Injection location	Intact loop cold leg (Spool piece 14)	
Actuation Pressure (kPa, gage)	4137	4274
Liquid volume (L)	80.1	79
Injection rate (FTU-ACC-1) (L/min)	87	95
N_2 flow duration (sec)	24	22
Accumulator CI-T-2 (Broken loop)		
Location	Broken loop cold leg (Spool piece 42)	
Actuation Pressure (kPa, gage)	4137	4480
Liquid volume (L)	16.4	14.7
Injection rate (FTB-ACC2) (L/min)	28.65	31
Accumulator CI-T-3 (Unbroken loop hot leg)		
Injection location	Intact loop hot leg (Spool piece 6)	
Temperature (TFU-SGS3-B) (°K)	547	542
Initial pressure (PU-SG3-T) (kPa, gage)	7584	7446
Liquid volume (L)	144.4	138
Injection rate (FTU-SGS-H) (L/min)	42.8 $\pm$ 4	40.7
Air actuated valve		
Open (seconds after rupture)	40	40
Close (seconds after rupture)	242	242

TABLE I (Cont'd)

TEST AND PRERUPTURE CONDITIONS FOR TEST S-28-1

ECC System	Specified Condition	Test Condition
Steam generator secondary fluid discharge		
Initial liquid level (cm)	295	286
Flow rate (L/min)	42.8 ± 4	42.9
Air actuated valve		
Opening time (sec)	40	39
Closing time (sec)	242	243
Intact loop LPIS		
Location	Cold leg (Spool piece 14)	
Actuation Pressure (kPa, gage)	1034	1014
Injection rate (FTU-LPIS) (L/min)	15.1	17.8
Broken loop LPIS		
Location	Cold leg (Spool piece 42)	
Actuation pressure (kPa, gage)	1034	1034
Injection rate (FTB-LPIS) (L/min)	3.6	4.4
Intact loop HPIS		
Location	Cold leg (Spool piece 14)	
Actuation pressure (kPa, gage)	12411	12400
Injection rate (FTU-HPIS) (L/min)	1.17	10.2
Broken loop HPIS		
Location	Cold leg (Spool piece 42)	
Actuation pressure (kPa, gage)	12411	12400
Injection rate (FTB-HPIS) (L/min)	0.38	1.1

TABLE II

TEST AND PRERUPTURE CONDITIONS FOR TEST S-28-2

Primary System	Specified Condition	Test Condition
Core power (AMPCORR-T) (VOLTCOR-T)	1.44	1.46
System pressure (PV ± 10) (kPa, gage)	15513 ± 172	15237
Loop temperature		
Intact loop cold leg (RBU-14) (°K)	557.8 ± 1	558
Intact loop hot leg (RBU-2) (°K)	594.4 ± 1	594
Broken loop hot leg (TFB-30) (°K)	591.7 ± 3	591
Core flow rate (FTV-COREIN) (L^3/min)	562 ± 18	560
Pressure suppression system		
Tank water temperature (TF-PSS-33) (°K)	Ambient	291
Tank water pressure (P-PSS) (kPa, gage)	155 ± 7	143
Pressurizer water (DPU-PRESLL) (kg)	9.07	9.52
Steam generator feedwater temperature (TRU-SGFW) (°K)	497 ± 6	478
Steam generator secondary liquid level (DPU-SG-SEC) (m)	295 ± 5	287

TABLE II (contd)

TEST AND PRERUPTURE CONDITIONS FOR TEST S-28-2

ECC System	Specified Condition	Test Condition
Accumulator CI-T-1 (Unbroken loop)		
Injection location	Intact loop cold leg (Spool piece 14)	
Actuation Pressure (kPa, gage)	4137	4180
Liquid volume (L)	80.1	82
Injection rate (FTU-ACC-1) (L/min)	87	90
N_2 flow duration (sec)	24	21
Accumulator CI-T-2 (Broken loop)		
Location	Broken loop cold leg (Spool piece 42)	
Actuation Pressure (kPa, gage)	4137	4250
Liquid volume (L)	16.4	10.8
Injection rate (FTB-ACC2) (L/min)	28.65	26
Accumulator CI-T-3 (Unbroken loop hot leg)		
Injection location	Intact loop hot leg (Spool piece 6)	
Temperature (TFU-SGS3-B) (°K)	547	541
Initial Pressure (PU-SG3-T) (kPa, gage)	7584	7446
Liquid volume (L)	144.4	144
Injection rate (FTU-SGS-H) (L/min)	4.28 $\pm$ 0.4	4.54
Air acutated valve		
Open (Seconds after rupture)	40	40
Close (Seconds after rupture)	Remains open	Remains open

TABLE II (contd)

TEST AND PRERUPTURE CONDITIONS FOR TEST S-28-2

ECC System	Specified Condition	Test Condition
Steam generator secondary fluid discharge		
Initial liquid level (cm)	295 ± 5	287
Flow rate (L/min)	4.28 ± 0.4	4.39
Air actuated valve		
Opening time (sec)	40	40
Closing time (sec)	Remains open	Remains open
Intact loop LPIS		
Location	Cold leg (Spool piece 14)	
Actuation pressure (kPa, gage)	1034	∿1200
Injection rate (FTU-LPIS) (L/min)	15.1	17.8
Broken loop LPIS		
Location	Cold leg spool piece 42)	
Actuation pressure (kPa, gage)	1034	∿1100
Injection rate (FTB-LPIS)	3.6	4.3
Intact loop HPIS		
Location	Cold leg (Spool piece 14)	
Actuation pressure (kPa, gage)	12411	∿12000
Injection rate (FTU-HPIS) (L/min)	1.17	9.4
Broken loop HPIS		
Location	Cold leg (Spool piece 42)	
Actuation pressure (kPa, gage)	12411	∿12000
Injection rate (FTB-HPIS) (L/min)	0.38	1.30

predictions through the period of the steam generator tube rupture injection until core quenching occurred. The analysis technique used in the test predictions is described in References 3 and 4. Selected comparisons between test predictions and test data are included in this report.

Test Results

The following discussion presents results of a preliminary evaluation of the effect of simulated steam generator tube ruptures on the core and system response during Tests S-28-1 and S-28-2. In considering the sensitivity of the peak rod cladding temperatures to the magnitude of the steam generator secondary-to-primary flow rate, Tests S-28-1 and S-28-2 represent two distinct regimes of core thermal-hydraulic response. In Test S-28-1, a negative core flow existed during the entire period of steam generator tube rupture flow. The strong negative core flow during this period was due to the comparatively large secondary-to-primary flow rate of 0.54 kg/s (equivalent to the flow associated with the single-ended rupture of 60 tubes in a PWR steam generator). In Test S-28-2, however, positive core flow persisted during most of the steam generator tube rupture injection period, despite the increased steam binding problem in the intact loop associated with the relatively small secondary-to-primary flow rate of 0.054 kg/s (equivalent to the flow associated with the single-ended rupture of only 6 tubes in a PWR steam generator).

Because of the differences in the core hydraulic response during the steam generator injection period for Tests S-28-1 and S-28-2, significant differences in the core thermal response were observed. Thus to facilitate a complete discussion of the effects of the magnitude of the steam generator secondary-to-primary flow on the core thermal-hydraulic response (as well as on the overall system response), results from Tests S-28-1 and S-28-2 are presented in separate sections. The first section discusses the overall system response and the core response for Test S-28-1, while the second section provides a similar discussion for Test S-28-2. Where applicable, results from Tests S-28-1 and S-28-2 are compared with data from the Series 28 baseline test, Test S-04-6. A final section presents comparisons of data for Tests S-28-1 and S-28-2 with selected results from the pretest calculations.

System and Core Response During Test S-28-1

The primary objective of Test S-28-1 was to determine the effect on the system and core response of a relatively large steam generator secondary-to-primary flow initiated at the start of refill, and in so doing, to establish a basis for determining and upper limit on the range of steam generator tube ruptures for which high rod cladding temperatures could

occur[a]. An analysis of the data from Test S-28-1 has provided insight into the phenomena which occur in the Semiscale Mod-1 system as a result of the rupture of a comparatively large number of steam generator tubes during the refill phase of a loss-of-coolant test. The first part of the following discussion is concerned with an evaluation of the behavior of the system in Test S-28-1 prior to the initiation of the steam generator tube rupture injection in order to establish similarity with the baseline Test S-04-6. The second section is concerned with an evaluation of the overall system hydraulic response both during and following the steam generator tube rupture injection. The third part deals primarily with the core thermal response following the initiation of steam generator tube rupture flow.

Initial Blowdown Behavior. The system conditions preceding the initiation of the steam generator tube rupture injection in Test S-28-1 were examined to determine if there were significant differences in the blowdown response between Tests S-28-1 and S-04-6. A comparison of data for the two tests indicates that minor differences in the system blowdown response did exist. The differences in the blowdown response are attributed to the failure of a valve in the hot leg heatup bypass line in Test S-28-1[b] and to a delay in the initiation of the core power decay of about 1 second in Test S-28-1 (as compared to Test S-04-6).

A comparison of the intact loop and core hydraulic response during the blowdown period for Test S-28-1 and S-04-6 illustrates the effect of the failure of the valve in the heatup bypass line. Figure 6 compares the fluid density in the intact loop just upstream of the location where the heatup bypass line connects to the hot leg. As indicated in the figure, the fluid density is substantially higher for Test S-28-1 between about

---

[a] The scaling analysis for Test Series 28 indicated that high rod cladding temperatures could occur in the Semiscale Mod-1 core only for secondary-to-primary flow rates equivalent to the flow associated with the single-ended rupture of a total of between about 10 and 60 tubes in 3 of 4 steam generators in a 4 loop PWR. (For comparison, note that the four-loop Trojan PWR has approximately 3300 tubes in each of the four steam generators). For secondary-to-primary flows equivalent to the flow from more than 60 tube ruptures, the analysis indicates good core cooling exists during the injection period, thus preventing high cladding temperatures.

[b] The existance of the failed valve in the hot leg heatup bypass line was not discovered until after Tests S-28-1 and S-28-2 had been run. The valve failure occurred in both tests and may have resulted in the injection of approximately 2.54 kg of liquid at about 589°K into the intact loop hot leg (spool 6) during blowdown.

10 and 40 seconds[a]. Since during this period the flow direction is toward the vessel and down through the core, the higher intact loop hot leg density indicates that the quality of the fluid entering the top of the heated section of the core is considerably lower for Test S-28-1 than for Test S-04-6. A comparison of the fluid temperatures in the intact loop hot leg near the vessel also indicates a lower quality fluid in the upper part of the core. Figure 7 compares the fluid temperatures near the vessel for Tests S-28-1 and S-04-6 and indicates that saturated fluid was entering the vessel in Test S-28-1 during the period between 10 and 40 seconds, while for Test S-04-6 considerable fluid superheat existed.

As a result of the somewhat lower quality fluid in the core for Test S-28-1, a higher rate of steam generation occurred than for Test S-04-6. The higher rate of steam generation, in turn, caused a substantially higher reverse core flow and a somewhat slower depressurization during the period between 20 and 40 seconds. Figure 8 compares the core inlet volumetric flow rates for the two tests, while Figure 9 compares the system pressure responses. These figures illustrate the effect of the different rates of steam generation in the core, due to the blowdown of the hot leg heatup bypass line.

An examination of the rod cladding temperature responses during blowdown inicates that the average peak cladding temperatures were between 50 and 60°K hotter for Test S-28-1 than for Test S-04-6. The hotter cladding temperatures for Test S-28-1 were a result of the 1 second delay in the initiation of the core power decay (see Figure 4). However, due to the higher steam generation rate in the core for Test S-28-1, and the corresponding improvement in core cooling, the rod cladding temperatures at the initiation of the steam generator tube rupture injection were essentially the same for both tests. It is thus concluded that differences in the core and system response during blowdown between Tests S-28-1 and S-04-6 do not significantly effect the behavior of the system following the initiation of steam generator tube rupture flow.

System Response to a Relatively Large Steam Generator Secondary-to-Primary Flow. The initiation of the steam generator tube rupture flow for Test S-28-1 occurred at approximately 40 seconds after rupture. During the period of injection (until approximately 242 seconds), the secondary-to-primary flow was the dominant influence on the overall system and core hydraulic response. A comparison of the volumetric flow rates at various points in the system illustrates the effect of the secondary-to-primary flow. Figures 10 and 11 compare the volumetric flow rates in the intact loop hot leg near the vessel and at the entrance to the core for Tests S-28-1 and S-04-6. As indicated in these figures

[a] The higher density after 40 seconds for Test S-28-1 is due to the steam generator tube rupture injection.

the reverse flow through the intact loop hot leg and down through the core for Test S-28-1 became substantially more negative at the initiation of the secondary-to-primary flow, while for Test S-04-6 at about the same time (40 seconds) the core flow became positive indicating the initiation of refill.

The strong reverse flow through the core for Test S-28-1 continued until the initiation of nitrogen flow from the intact loop accumulator at about 68 seconds. During the duration of the accumulator nitrogen flow (until about 88 seconds) the core flow remained negative at a considerably reduced rate. Once the intact loop accumulator nitrogen flow ceased, however, the magnitude of the core flow did not increase to its value prior to the nitrogen injection even though the secondary-to-primary flow continued at essentially the same rate. This can be attributed to a change in the resistance to steam flow in the intact loop cold leg. During the period of accumulator liquid injection into the intact loop cold leg, steam flow from the hot leg to the vessel inlet side of the break was effectively blocked. The effect of the accumulator nitrogen flow, however, was to clear liquid from the intact loop cold leg. This phenomenon is illustrated in Figure 12 which shows the fluid density in the intact loop cold leg. Once the nitrogen flow ceased, an additional path for removal of steam from the intact loop occurred. The volumetric flow near the vessel on the vessel inlet side of the broken loop, shown in Figure 13, indicates the substantial increase in the flow rate for Test S-28-1 once the nitrogen flow ceased. As a result, the magnitude of the core inlet volumetric flow did not increase significantly, but remained substantially negative until the steam generator secondary-to-primary flow ceased at about 242 seconds.

The refill behavior of the vessel during the period of secondary-to-primary flow for Test S-28-1 was strongly dependent on the magnitude of the core reverse flow rate. Figure 14 compares the downcomer collapsed liquid level obtained from a downcomer differential pressure measurement for Tests S-28-1 and S-04-6. The figure indicates the relative rate of refill of the downcomer for the two tests. As shown in the figure, refill of the downcomer did not begin until about 110 seconds for Test S-28-1 (approximately the same time that the core reverse flow began to decrease). Partial refill of the downcomer and lower plenum after 110 seconds was accomplished by the intact loop low pressure injection system (LPIS). However, because of the strong reverse core flow, the lower plenum did not completely refill until after the steam generator secondary-to-primary flow stopped at about 242 seconds. Figure 15 compares the collapsed liquid levels obtained from a lower plenum-to-upper plenum differential pressure measurement for Tests S-28-1 and S-04-6. As indicated in the figure only a partial refill of the lower plenum occurred for Test S-28-1 until about 242 seconds, whereas for Test S-04-6 core reflood was occurring during the entire period. The increase in collapsed liquid level at 242 seconds for Test S-28-1

is a result of the cessation of the secondary-to-primary flow and corresponds to a reduction in the downcomer collapsed liquid level (Figure 14). Reflood of the core was initiated at about 255 seconds as indicated in Figure 16 which shows the core inlet fluid density for Test S-28-2.

In previous tests for which downcomer refill had not begun prior to the initiation of the intact loop accumulator nitrogen flow, the initiation of the nitrogen flow forced the start of refill. For Test S-28-1, however, the intact loop accumulator nitrogen flow had very little effect on the downcomer response other than to reduce the velocity of the upward flow in the downcomer. Figure 17 shows the downcomer fluid velocity at 1.016 m below the cold leg centerline and indicates the reduction in upward flow velocity at the initiation of nitrogen injection. A comparison of the fluid temperatures at 1.778 m and 3.962 m below the cold leg centerline in the downcomer for Test S-28-1 (Figure 18), indicates that penetration of some saturated fluid to the 1.778 m elevation did occur for Test S-28-1 at the initiation of the nitrogen flow. However, the upward steam flow in the downcomer was sufficient to prevent the initiation of refill until about 110 seconds.

Core Thermal Response for a Relatively Large Steam Generator Secondary-to-Primary Flow. The core thermal response for Test S-28-1 was characterized by a rapid top-down quench of the entire core following the initiation of the steam generator secondary-to-primary injection. Figures 19, 20, and 21 show the rod cladding temperatures at various elevations in the core for rods F5, F4, and A4 respectively, and illustrate the top-down quench behavior. For comparison purposes, Table III provides the quench times at each thermocouple location in the core for Tests S-28-1 and S-04-6. As indicated in the table, most thermocouple locations in the core for Test S-28-1 quenched between 45 and 90 seconds, while some thermocouple locations in the lower section of the core did not quench until between 100 and 180 seconds. This is compared to the bottom-top-middle quench behavior with quench times ranging from 62 to 295 seconds for Test S-04-6. Figure 22 graphically illustrates the results presented in Table III. The figure indicates whether the quench times were obtained from high power rods or low power rods, and whether or not the rods were adjacent to an unpowered rod location.

As a result of the strong reverse core flow and the relatively low quality fluid entering the vessel at the vessel outlet side of the intact loop in Test S-28-1 (see Figure 23), the maximum rod cladding temperatures during the period of secondary-to-primary flow occurred at the initiation of the injection, and were considerably lower than the maximum cladding temperatures during the blowdown period. Table IV lists the maximum core cladding temperatures and the times at which the maximums occur for each thermocouple location in the core for Test S-28-1. For comparison purposes similar results for Test S-04-6 are included. As indicated in Table IV most cladding temperature maximums for Test S-28-1 occur during blowdown whereas for Test S-04-6 most cladding temperature maximums occur after the start of reflood.

TABLE III

Core Quench Times for Tests S-28-1 and S-04-6

Thermocouple I. D.	Test S-28-1 (sec)	Test S-04-6 (sec)
E3-05	94	77
C7-07	124	86
F2-07	147	84
E6-08	111	88
A4-09	99	95
E4-09	91	93
G3-13	115	108
D2-14	106	109
D4-14	78	103
E8-14	184	107
F4-14	75	106
G5-14	100	111
C7-15	110	135
C4-20	78	NA
D7-20	122	191
E2-20	121	184
E3-20	77	97
E5-20	77	115
F5-20	78	112
D1-21	112	140
F2-22	145	106
E3-24	43	106
G5-24	81	208
D6-25	83	195
F2-25	122	196
E5-25	71	184
C4-26	67	208
D8-26	73	217
F5-26	66	202
E4-27	67	236
C5-28	59	220
E6-28	78	201
A4-29	69	229
A5-29	71	230
B5-29	59	236
B6-29	74	188
D3-29	63	242
D4-29	64	227
E8-29	131	234

TABLE III (Contd)

Thermocouple I. D.	Test S-28-1 (sec)	Test S-04-6 (sec)
F4-29	58	238
G4-29	66	240
B3-32	63	98
H5-32	72	294
B5-33	51	183
E1-33	94	184
E2-33	82	248
F5-33	56	265
G4-33	60	277
E6-37	63	107
C2-28	56	80
G4-38	57	269
A4-39	50	NA
D3-39	53	85
E7-44	73	298
F4-44	50	99
A5-45	47	99
C4-53	45	298
C6-53	50	63
F5-53	50	68
E4-55	46	71
D2-61	63	78

TABLE IV

Maximum Core Cladding Temperatures and Times at
Which Maximum Temperatures Occur for
Tests S-28-1 and S-04-6

Thermocouple I. D.	Test S-28-1 °K (sec)	Test S-04-6 °K (sec)
E3-05	730 (39)	710 (44)
C7-07	864 (39)	840 (44)
F2-07	767 (39)	765 (52)
E6-08	822 (10)	808 (53)
A4-09	928 (10)	885 (9)
E4-09	807 (39)	863 (10)
G3-13	904 (10)	890 (64)
D2-14	965 (10)	902 (64)
D4-14	899 (10)	860 (64)
E8-14	975 (9)	935 (64)
F4-14	881 (10)	885 (64)
G5-14	908 (10)	921 (58)
C7-15	955 (10)	943 (64)
C4-20	913 (10)	NA
D7-20	1010 (10)	966 (9)
E2-20	924 (10)	891 (58)
E3-20	910 (10)	846 (54)
E5-20	951 (10)	903 (54)
F5-20	906 (10)	888 (54)
D1-21	1125 (10)	1066 (9)
F2-22	1003 (10)	NA
E3-24	1033 (45)	934 (64)
G5-24	970 (10)	982 (62)
D6-25	971 (10)	959 (64)
F2-25	969 (10)	936 (64)
F5-25	968 (10)	959 (64)
C4-26	980 (10)	NA
D8-26	872 (9)	NA
F5-26	963 (10)	NA
E4-27	938 (10)	934 (71)
C5-28	943 (10)	948 (71)
E6-28	945 (10)	940 (64)
A4-29	1058 (10)	NA
A5-29	1123 (9)	1075 (9)
B5-29	971 (10)	NA
B6-29	1064 (9)	1048 (8)
D3-29	964 (10)	918 (71)
D4-29	939 (10)	914 (71)

TABLE IV (Contd)

Thermocouple I. D.	Test S-28-1 °K (sec)	Test S-04-6 °K (sec)
E8-29	999 (10)	997 (71)
F4-29	940 (10)	940 (71)
G4-29	953 (10)	968 (71)
B3-32	875 (10)	819 (9)
H5-32	906 (9)	946 (71)
B5-33	871 (10)	856 (84)
E1-33	907 (10)	819 (162)
E2-33	926 (10)	884 (182)
F5-33	863 (9)	916 (71)
G4-33	894 (10)	921 (70)
E6-37	780 (10)	810 (60)
C2-38	779 (11)	691 (72)
G4-38	748 (10)	853 (64)
A4-39	808 (10)	NA
D3-39	791 (10)	715 (75)
E7-44	656 (0)	768 (189)
F4-44	675 (10)	703 (84)
A5-45	677 (13)	692 (8)
C4-53	618 (0)	619 (0)
C6-53	638 (0)	638 (0)
F5-53	613 (0)	609 (0)
E4-55	631 (0)	633 (0)
D2-61	608 (0)	608 (0)

Once quenching occurred in Test S-28-1, the cladding temperatures remained near the fluid saturation temperature, until cessation of the secondary-to-primary injection. The cessation of the steam generator tube rupture flow resulted in a reduction of the core flow to zero, which in turn caused dryout of the core heater rods and a resulting gradual increase in the rod cladding temperatures. However, the reflood of the core by LPIS flow (initiated at about 255 seconds) was sufficient to requench the core by about 300 seconds (Figures 19 through 21). The maximum cladding temperatures resulting from the dryout did not exceed 620°K.

System and Core Response During Test S-28-2

The primary objective of Test S-28-2 was to determine the effect on the system and core response of a small steam generator secondary-to-primary flow initiated at the start of refill, and in so doing to establish a basis for determining a lower limit on the range of steam generator tube ruptures for which high rod cladding temperatures could occur. An analysis of the data from Test S-28-2 has been performed to evaluate the effect of the small secondary-to-primary flow on the thermal-hydraulic response of the system and core. Results of the analysis are presented in two sections. The first section deals with the effect of the secondary-to-primary flow on the overall system hydraulic response. The second section is primarily concerned with the core thermal response following the initiation of the steam generator tube rupture. Where applicable, the data from Test S-28-2 are compared to results from the baseline test, Test S-04-6.

As in Test S-28-1, the failure of a valve in the heatup bypass line during the early part of blowdown for Test S-28-2 caused some minor differences in the core thermal-hydraulic response between Tests S-28-2 and S-04-6. At the initiation of the secondary-to-primary injection (at about 40 seconds), the core cladding temperatures were an average of approximately 60°K cooler for Test S-28-2 than for Test S-04-6. Thus it is expected that the core cladding temperatures during the secondary-to-primary injection phase of Test S-28-2 are somewhat cooler than would have occurred if the blowdown of the heatup bypass line had not occurred.

System Response to a Small Steam Generator Secondary-to-Primary Flow

The steam generator tube rupture flow for Test S-28-2 was initiated at about 40 seconds after rupture and continued for the duration of the test. Comparisons of the volumetric flow rates at various points in the system illustrate the effect of the small secondary-to-primary flow on the overall system and core hydraulic response. Figures 24 and 25 compare the volumetric flow rates in the intact loop hot leg near the vessel and at the entrance to the core for Tests S-28-2 and S-04-6. As indicated in these figures, the flow at both locations became substantially more negative at the initiation of the steam generator tube rupture flow for Test S-28-2. As mentioned previously, the flow reversal at both stations at about 40 seconds for Test S-04-6 is indicative of the initiation of vessel refill.

The core flow and corresponding downcomer flow remained negative for Test S-28-2 until the initiation of the intact loop accumulator nitrogen flow at about 66 seconds. As a result, the vessel refill for Test S-28-2 was not initiated until the accumulator nitrogen injection began (as compared to Test S-04-6 for which vessel refill had been initiated prior to the intact loop accumulator nitrogen flow). Figure 26 compares the downcomer collapsed liquid level obtained from a downcomer differential pressure measurement for Tests S-28-2 and S-04-6. As indicated in the figure, the downcomer collapsed liquid level for Test S-28-2 did not begin to increase until shortly following the initiation of accumulator nitrogen injection (at about 66 seconds), whereas for Test S-04-6, the downcomer was essentially refilled prior to the initiation of nitrogen flow (at about 68 seconds). The considerable increase in the downcomer collapsed liquid level at about 70 seconds for Test S-28-2 is due primarily to penetration into the downcomer of ECC fluid stored in the vessel inlet annulus and upper portion of the downcomer during the downcomer countercurrent phase of the test. The relatively slow refill of the downcomer for Test S-28-2 (as well as for Test S-04-6) after about 100 seconds was accomplished by the intact loop LPIS.

As a result of the longer downcomer countercurrent flow period for Test S-28-2 (caused by the steam generator secondary-to-primary flow) which caused a later initiation of vessel refill, core reflood did not begin until about 80 seconds, as compared to about 58 seconds for Test S-04-6. Figure 27 compares the core inlet fluid density for Tests S-28-2 and S-04-6 and illustrates the delay in initiation of reflood for Test S-28-2. Because of the delay in initiation of reflood for Test S-28-2, the core reflood rate prior to 100 seconds was considerably lower than in Test S-04-6 for which accumulator refill of the downcomer had occurred. Figure 28 compares the core collapsed liquid level obtained from a lower plenum-to-upper plenum differential pressure measurement for Tests S-28-2 and S-04-6. The figure illustrates the effect of the small secondary-to-primary flow into the intact loop on the core reflood behavior. Although the steam generator injection had a considerable effect on the core reflood behavior early in the injection period, it did not significantly effect the reflood rate later in the test.

Core Thermal Response to a Small Steam Generator Secondary-to-Primary Flow. The effect of a small steam generator secondary-to-primary flow on the core thermal response is illustrated by a comparison of rod cladding temperatures at several elevations in the core for Tests S-28-2 and S-04-6. Figures 29 through 33 compare typical rod cladding temperatures at the 0.38, 0.53, 0.74, and 0.97 m elevations in the core for the two tests. As indicated in the figures considerable differences in the core thermal behavior occurred. These differences can be attributed to the changes in the system and core hydraulic behavior as a result of the steam generator injection in Test S-28-2. In Test S-04-6, downcomer refill and the initiation of core reflood occurred prior to the injection of nitrogen from the intact loop accumulator. The effect of the nitrogen injection (at about 68 seconds) was to cause the addition of a considerable

quantity of liquid to the lower part of the core (see Figure 28). The addition of the liquid to the lower core volume, in turn, caused an increase in the steam generation in the lower part of the core, and a corresponding increase in steam flow up through the core. As a result, the core cladding temperatures turned over shortly after the initiation of the accumulator nitrogen flow, and exhibited the period of improved cooling observed in Figures 29 through 33.

For Test S-28-2, however, downcomer refill was initiated by the injection of accumulator nitrogen flow, and the core reflood initiation was accomplished with the intact loop LPIS flow. Thus the initial core reflood rate for Test S-28-2 was considerably lower and resulted in the addition of considerably less fluid to the core volume than occurred for Test S-04-6. As a result, the turnover in cladding temperatures following the initiation of reflood for Test S-28-2 occurred only in the bottom 1/3 of the core (Figures 29 and 30), while the cladding temperatures in the upper 2/3 of the core exhibited a gradual heatup (Figures 31 through 33). The relatively low reflood rate for Test S-28-2 (Figure 28), however, was sufficient to cause the core cladding temperatures in the upper 2/3 of the core to turn over by about 150 seconds. As indicated previously, the steam generator injection during the period following 100 seconds does not appear to have affected the core reflood rate.

A comparison of the rod quench times for Tests S-28-2 and S-04-6 further illustrates the effect of the steam generator secondary-to-primary flow on the core thermal response. Table V lists the quench times for all thermocouple locations for the two tests. As indicated in the table, the quench times for Test S-28-2 in the lower 1/3 of the core were somewhat delayed as compared to Test S-04-6, while the quench times in the middle 1/3 of the core were approximately the same for both tests. The delay of quenching of the lower 1/3 of the core for Test S-28-2 corresponds directly to the somewhat delayed initiation of reflood. The major difference in quench times occurred in the upper 1/3 of the core. As indicated in the table, the quench times for Test S-28-2 were considerably later than for Test S-04-6. This can be attributed to the fact that, because of the relatively slow reflood rate in Test S-28-2, very little fluid entrainment occurred. For Test S-04-6, however, the core reflood rate was considerably higher than for Test S-28-2 during the early portion of the reflood phase. As a result, sufficient liquid was entrained in the steam flow up through the core to cause early quenching of the rods in the upper section of the core. Figure 34 graphically illustrates the quench time results presented in Table V.

A comparison of the peak cladding temperatures and the times at which the peak cladding temperatures occurred for Tests S-28-2 and S-04-6 indicates that the effect of the steam generator injection was to shift the times of the peak temperatures to later in the reflood period, although the magnitude of the peak temperatures were similar for both tests. Table VI lists the peak cladding temperatures and the times at which the peak temperatures occur for each thermocouple location for

TABLE V

Rod Quench Times for Tests S-28-2 and S-04-6

Thermocouple I.D.	Test S-28-2 (sec)	Test S-04-6 (sec)
E3-05	92	77
C7-07	107	86
F2-07	102	84
E6-08	106	88
A4-09	120	95
E4-09	116	93
G3-13	145	108
D2-14	146	109
D4-14	142	103
E8-14	149	107
F4-14	142	106
G5-14	144	111
C7-15	161	135
C4-20	177	NA
D7-20	178	191
E2-20	174	184
E3-20	166	97
E5-20	175	115
F5-20	170	112
D1-21	183	140
F2-22	185	NA
E3-24	186	106
G5-24	192	208
D6-25	198	195
F2-25	207	196
F5-25	195	184
C4-26	207	NA
D8-26	260	NA
F5-26	202	202
E4-27	217	236
C5-28	215	220
E6-28	213	210
A4-29	229	NA
A5-29	228	230
B5-29	223	NA
B6-29	234	188
D3-29	220	242
D4-29	220	227

TABLE V (Contd)

Thermocouple I.D.	Test S-28-2 (sec)	Test S-04-6 (sec)
E8-29	223	234
F4-29	221	238
G4-29	221	240
B3-32	260	98
H5-32	264	294
B5-33	253	183
E1-33	263	184
E2-33	252	248
F5-33	251	265
G4-33	251	276
E6-37	223	107
C2-38	221	80
G4-38	246	269
A4-39	259	NA
D3-39	223	85
E7-44	309	298
F4-44	305	99
A5-45	322	99
C4-53	224	298
C6-53	240	63
F5-53	246	68
E4-55	349	71
D2-61	368	78

TABLE VI

Peak Core Cladding Temperatures and Times
at Which Peak Temperatures Occur For
Tests S-28-2 and S-04-6

Thermocouple I.D.	Test S-28-2 °K (sec)	Test S-04-6 °K (sec)
E3-05	736 (69)	710 (44)
C7-07	864 (67)	840 (44)
F2-07	779 (69)	765 (52)
E6-08	818 (69)	808 (53)
A4-09	901 (69)	885 (9)
E4-09	857 (10)	863 (10)
G3-13	874 (113)	890 (64)
D2-14	948 (10)	902 (64)
D4-14	850 (78)	860 (64)
E8-14	922 (8)	935 (64)
F4-14	853 (83)	885 (64)
G5-14	889 (69)	921 (58)
C7-15	928 (69)	943 (64)
C4-20	854 (69)	NA
D7-20	969 (9)	966 (9)
E2-20	947 (9)	891 (58)
E3-20	846 (9)	846 (54)
E5-20	883 (69)	903 (54)
F5-20	846 (9)	888 (54)
D1-21	1062 (8)	1066 (9)
F2-22	932 (9)	NA
E3-24	906 (113)	934 (64)
G5-24	925 (78)	982 (62)
D6-25	943 (123)	959 (64)
F2-25	894 (132)	936 (64)
F5-25	906 (9)	959 (64)
C4-26	924 (132)	NA
D8-26	940 (146)	NA
F5-26	914 (140)	NA
E4-27	916 (143)	934 (71)
C5-28	954 (141)	948 (71)
E6-28	920 (141)	940 (64)
A4-29	1029 (9)	NA
A5-29	1068 (9)	1075 (9)
B5-29	977 (132)	NA
B6-29	1092 (9)	1048 (8)
D3-29	904 (155)	918 (71)
D4-29	906 (155)	914 (71)

TABLE VI (Contd)

Thermocouple I.D.	Test S-28-2 °K (sec)	Test S-04-6 °K (sec)
E8-29	968 (132)	997 (71)
F4-29	913 (153)	940 (71)
G4-29	925 (151)	968 (71)
B3-32	879 (162)	819 (9)
H5-32	933 (151)	946 (71)
B5-33	950 (155)	856 (84)
E1-33	898 (151)	819 (162)
E2-33	905 (162)	884 (182)
F5-33	888 (172)	916 (71)
G4-33	900 (157)	921 (70)
E6-37	794 (145)	810 (60)
C2-38	766 (146)	691 (72)
G4-38	826 (151)	853 (64)
A4-39	857 (145)	NA
D3-39	810 (157)	715 (75)
E7-44	824 (180)	768 (189)
F4-44	808 (198)	703 (84)
A5-45	820 (180)	692 (8)
C4-53	654 (177)	619 (0)
C6-53	706 (168)	638 (0)
F5-53	690 (174)	609 (0)
E4-55	699 (176)	633 (0)
D2-61	631 (198)	608 (0)

Tests S-28-2 and S-04-6. For Test S-04-6 a majority of the peak cladding temperatures occurred shortly following the initiation of core reflood. However, for Test S-28-2 most of the peak cladding temperatures occurred considerably later during the reflood phase of the test. A core maximum temperature of 1092°K was observed for Test S-28-2 while the maximum temperature for Test S-04-6 was 1075°K.

Comparison of Selected Data to Calculations

Test predictions of the thermal-hydraulic response characteristics for Tests S-28-1 and S-28-2 were performed using the FLOOD4 computer code. Detailed descriptions of the analysis technique used in the calculations and additional predicted results for the two tests are given in References 3 and 4.

A comparison of the predicted and measured rod cladding temperatures for Test S-28-1 indicates that the FLOOD4 calculation considerably overpredicted the measured cladding temperatures during the reflood phase of the test. The peak calculated cladding temperature on the rod high power zone during reflood was about 1021°K, whereas the peak measured cladding temperature on the high power zone did not exceed 730°K during the reflood phase of the test. The substantial overprediction of the measured cladding temperatures can be attributed to the method of analysis used in the calculations. In the calculations for Test S-28-1 the transient was divided into four main time periods. These periods consisted of: (1) the blowdown period prior to the steam generator tube rupture, (2) a period of reverse core flow after the tube rupture and lasting until the steam generator secondary empties, (3) heatup of the core as the lower plenum is refilled by the HPIS and LPIS, and (4) core reflood by the LPIS and HPIS. For the second period described above a FLOOD4 calculation was performed to determine the core cooldown rate due to the steam generator tube rupture flow. However, to be conservative, the calculation purposely did not take into account the liquid portion of the flow through the core, and thus did not predict the quenching and corresponding low cladding temperatures obtained during Test S-28-1 (see Figures 19 through 21). As a result, the initial cladding temperatures calculated for the period of heatup and the corresponding initial temperatures calculated for the reflood period were considerably higher than the measured data.

The predicted and measured cladding temperatures for Test S-28-2 exhibited reasonably good agreement. The FLOOD4 calculation predicted a rod cladding temperature heatup in the middle of the rod high power step of only 9°K following the initiation of core reflood. This compares to measured rod cladding temperature heatups near the middle of the high power step of between about 5 and 15°K.

References

(1) H. S. Crapo, B. L. Collins, and K. E. Sackett, "Experiment Data Report for Semiscale Mod-1 Tests S-04-5 and S-04-6 (Baseline ECC Tests)", TREE-NUREG-1045, January 1977.

(2) D. J. Olson Ltr to P. E. Litteneker, DJO-125-77, "Transmittal of Semiscale EOS Appendix 28", June 1977.

(3) D. J. Olson Ltr to R. E. Tiller, DJO-136-77, "Test Prediction of Semiscale Mod-1 Integral Test S-28-1 (Revision 1)", June 13, 1977.

(4) D. J. Olson Ltr to P. E. Litteneker, DJO-132-77, "Test Prediction of Semiscale Mod-1 Integral Test S-28-2", June 8, 1977.

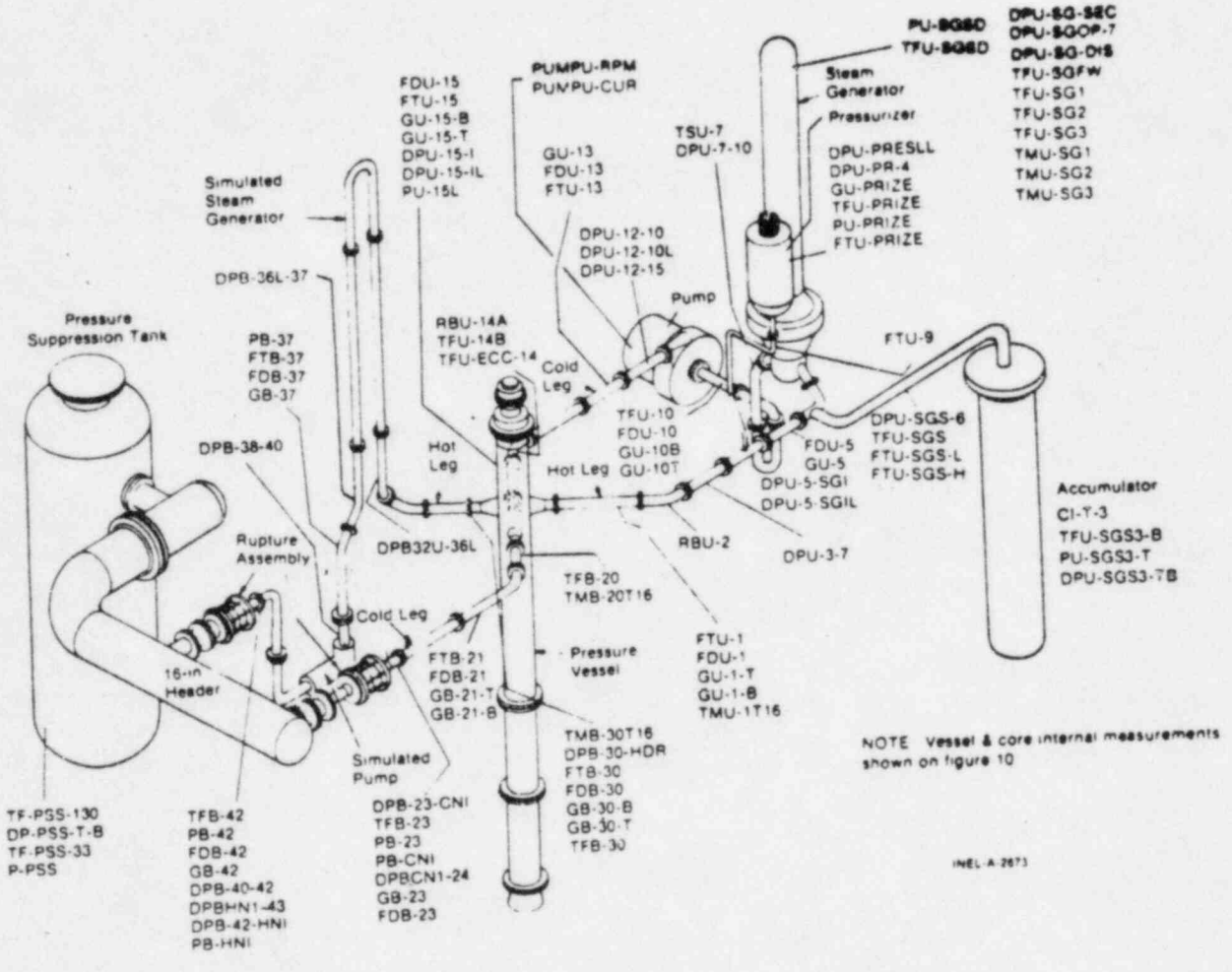

Figure 1. Semiscale Mod-1 System and Instrumentation for Cold Leg Break Configuration - Isometric

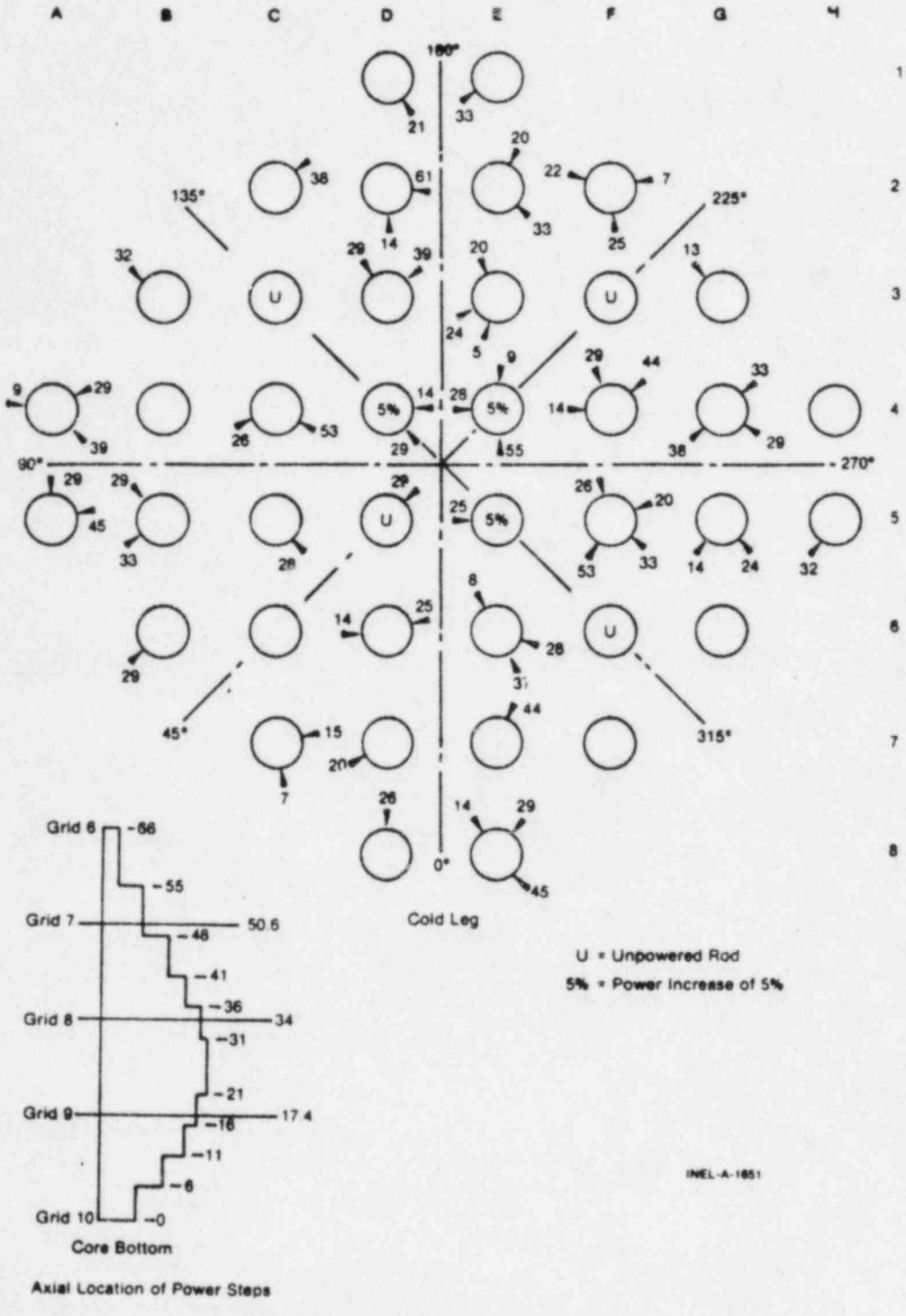

Figure 2. Semiscale Mod-1 Core - Plan View with Thermocouple Locations

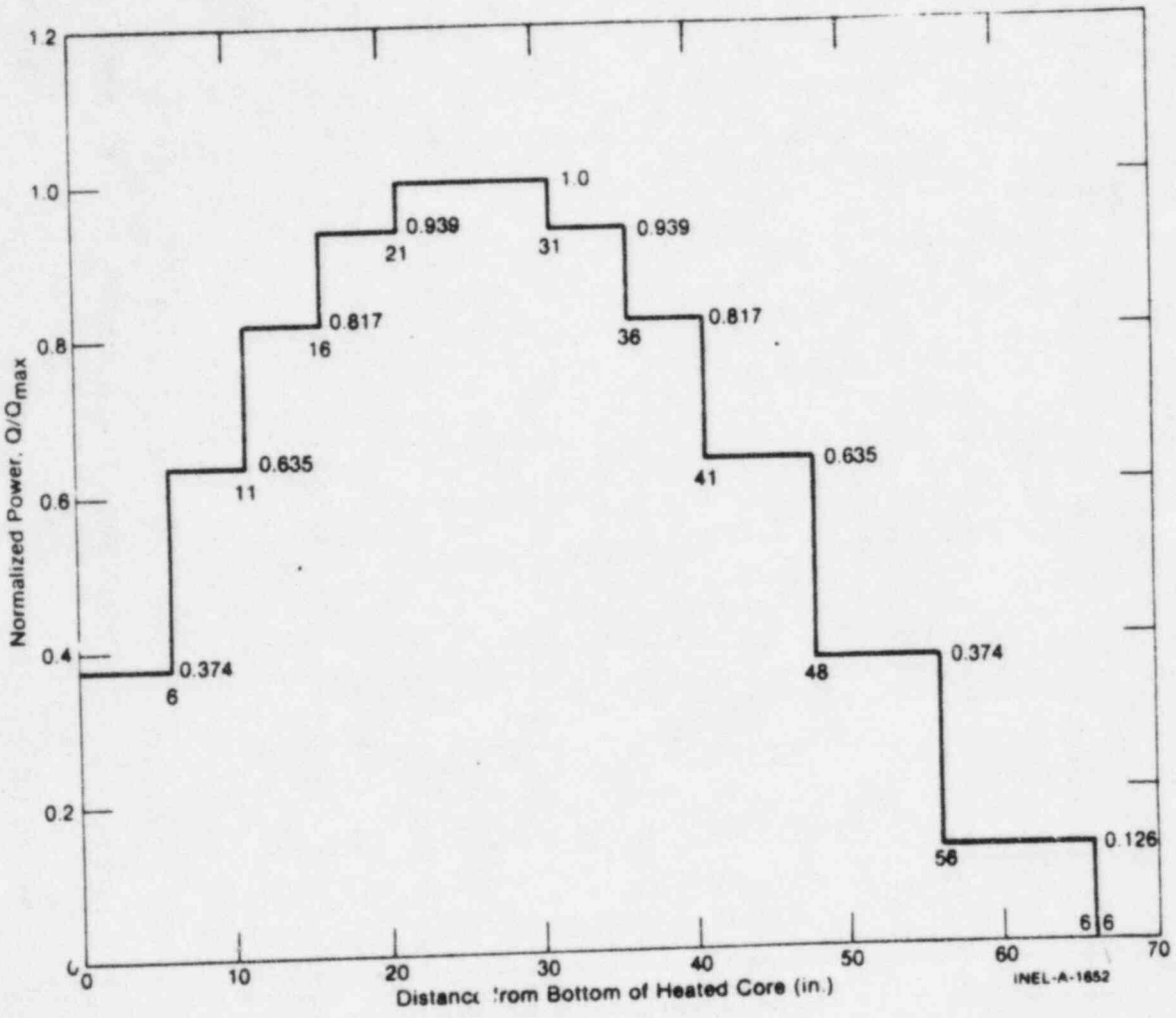

Figure 3. Semiscale Mod-1 Axial Power Profile

PRELIMINARY

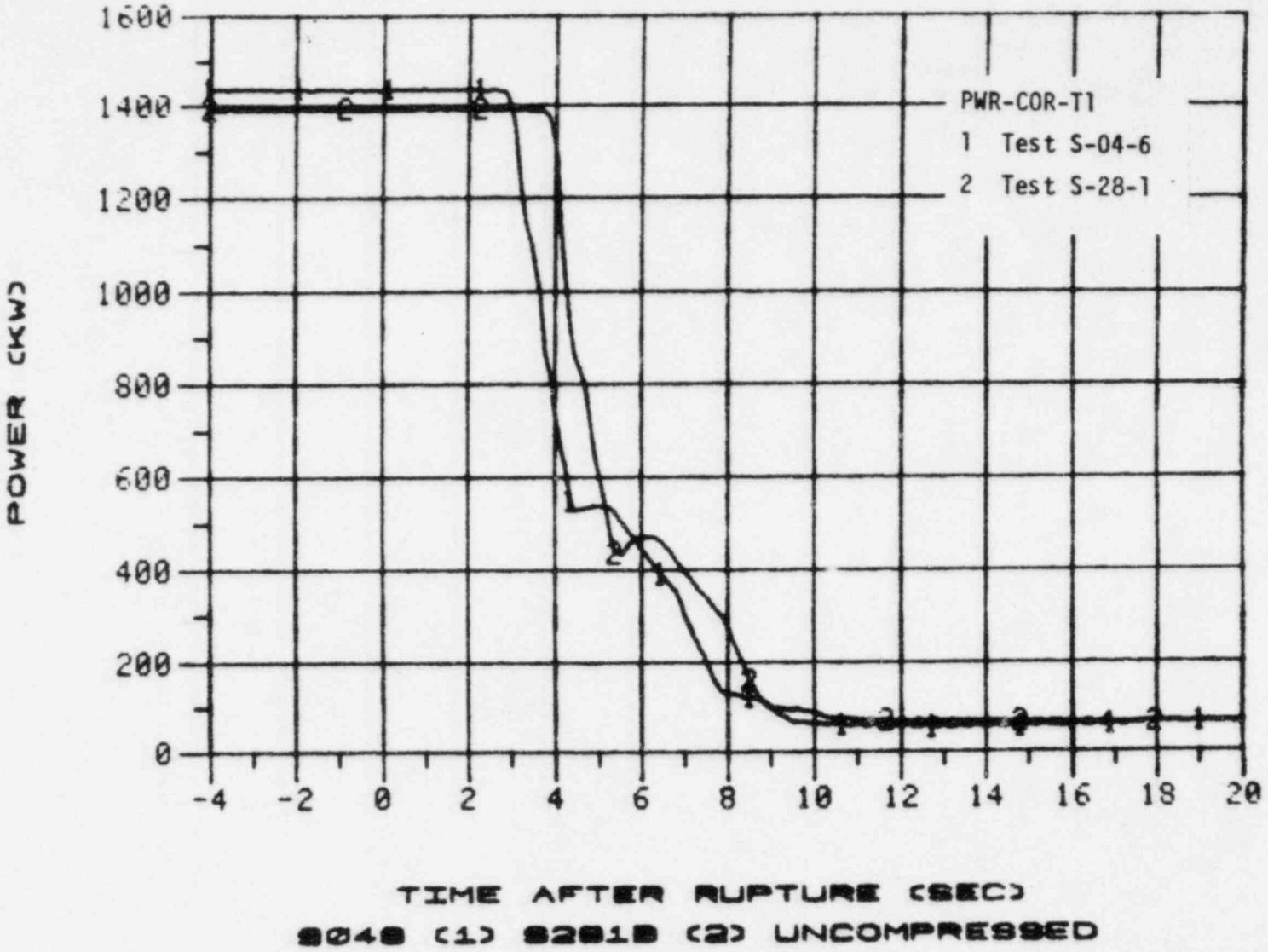

Figure 4. Initial Core Power Decay - Tests S-28-1 and S-04-6

PRELIMINARY

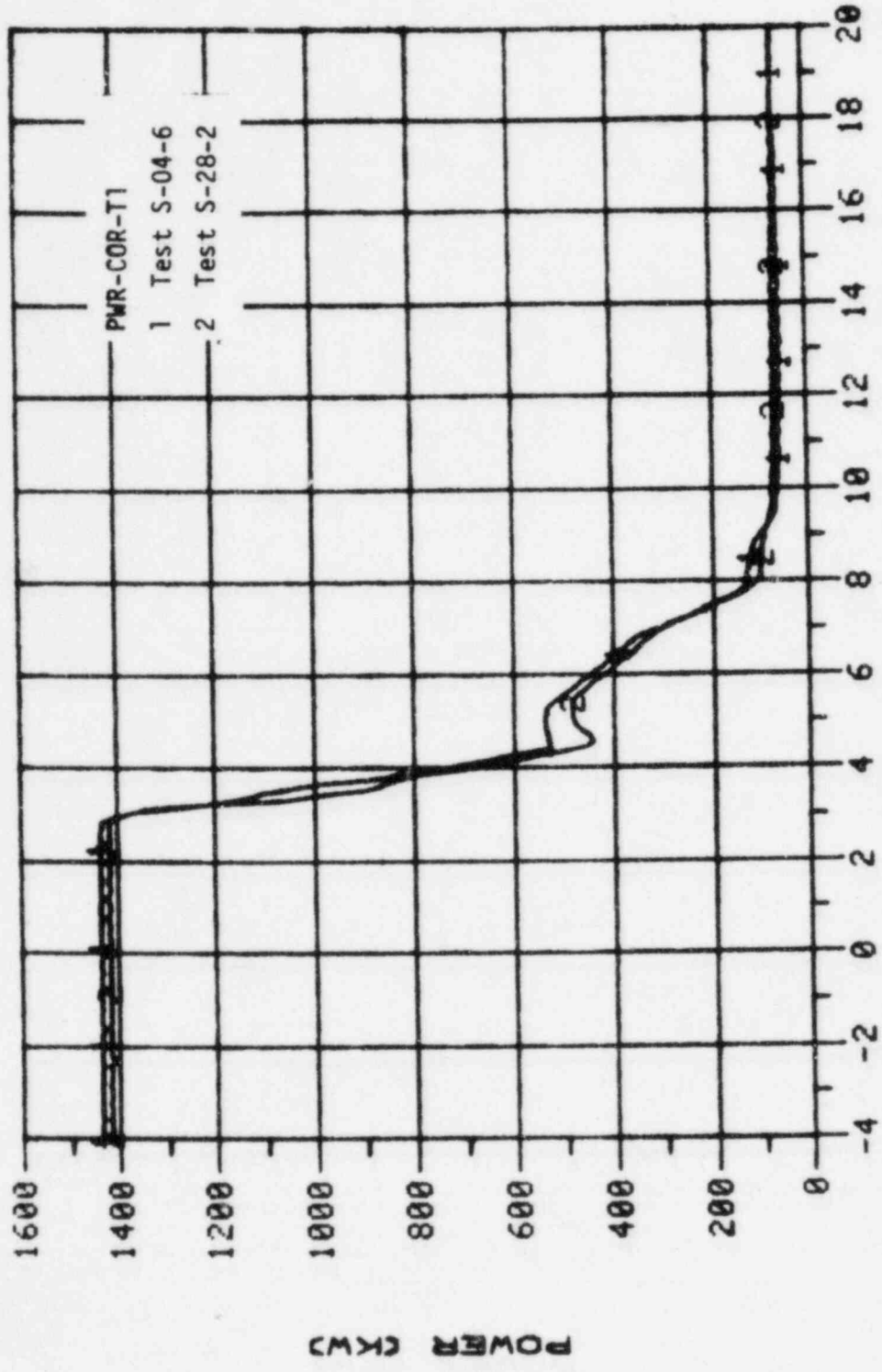

Figure 5. Initial Core Power Decay - Tests S-28-2 and S-04-6

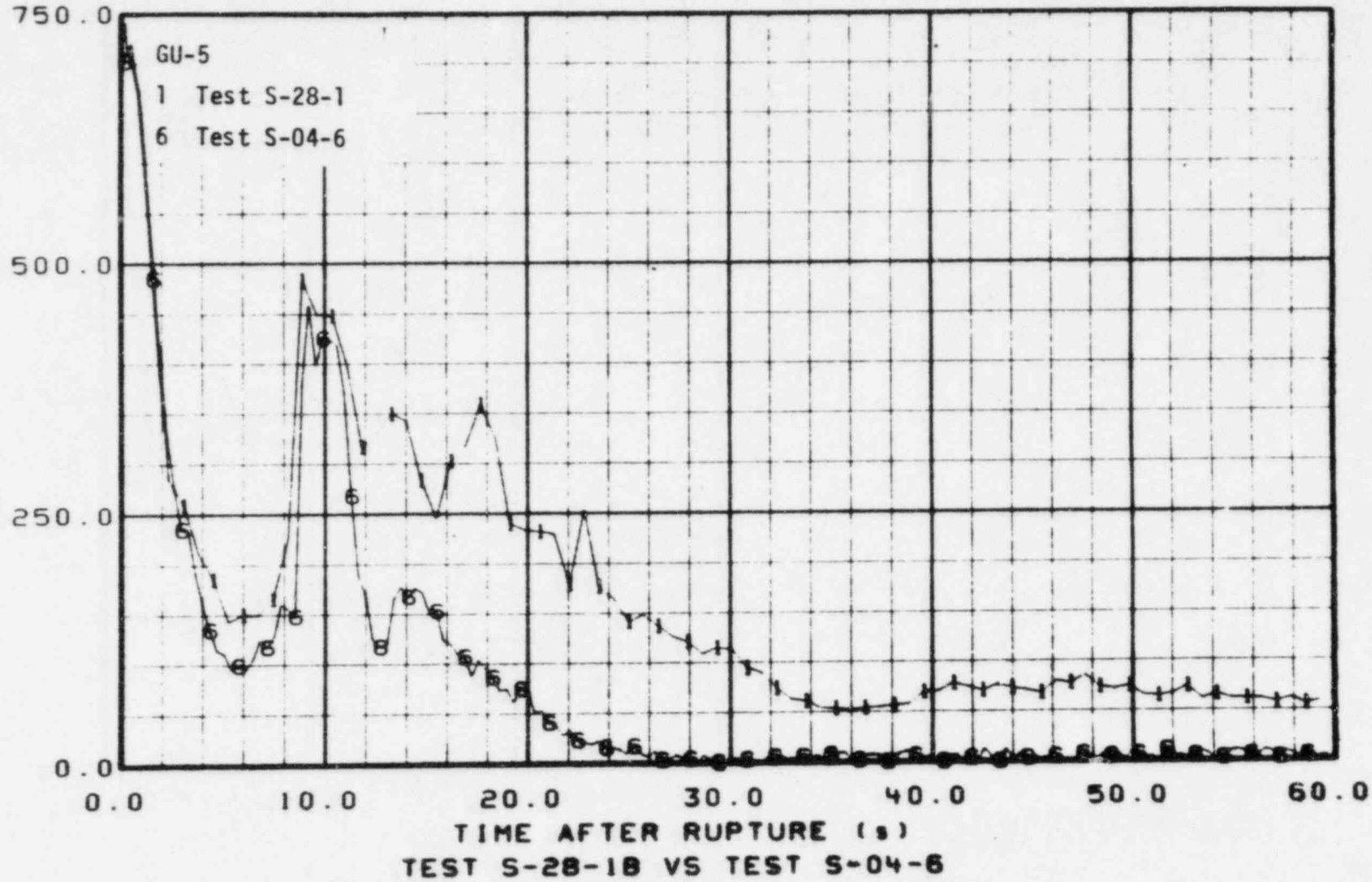

PRELIMINARY

PRELIMINARY

Figure 6. Comparison of Intact Loop Hot Leg Fluid Density - Tests S-28-1 and S-04-6

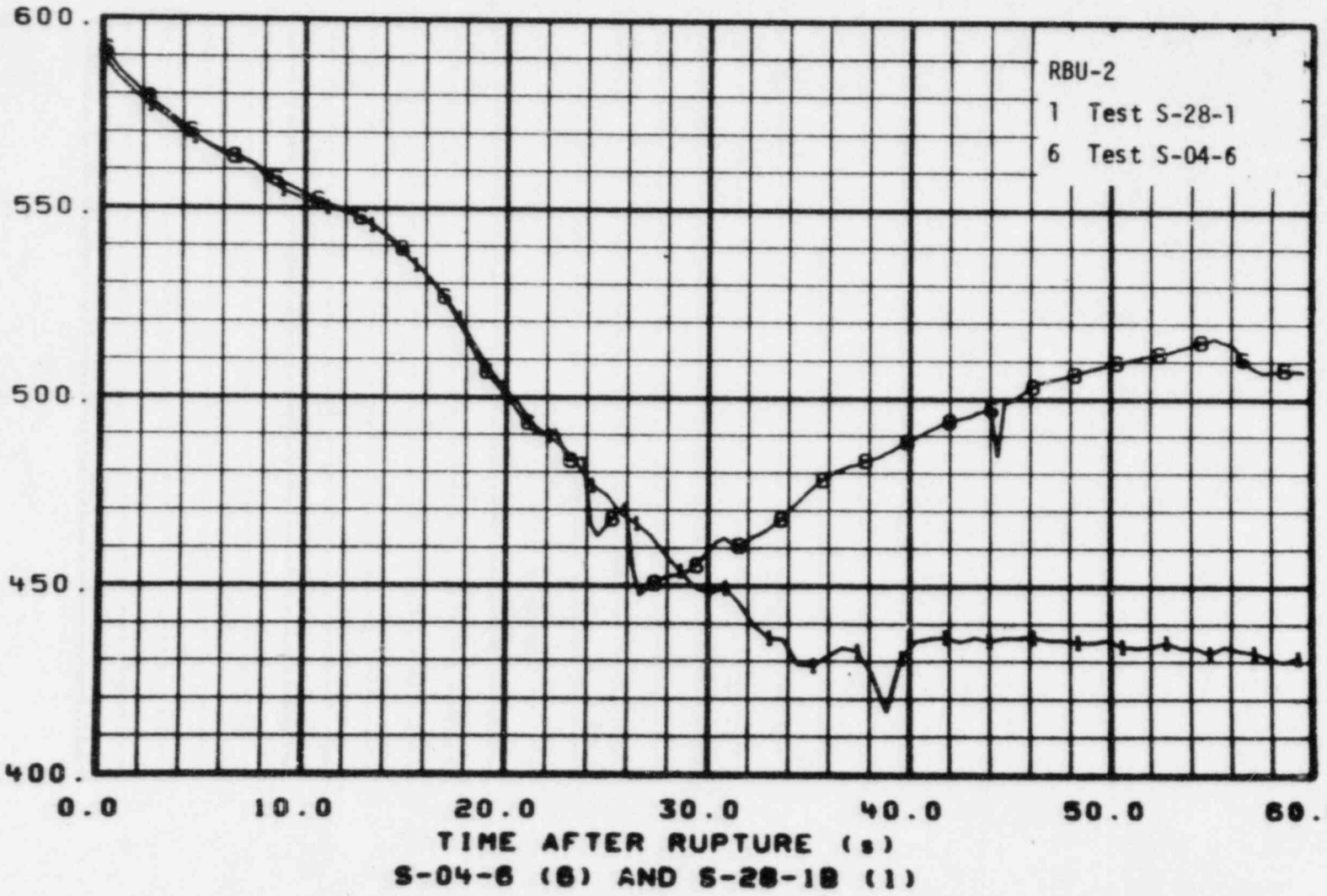

Figure 7. Comparison of Intact Loop Hot Leg Fluid Temperatures - Tests S-28-1 and S-04-6

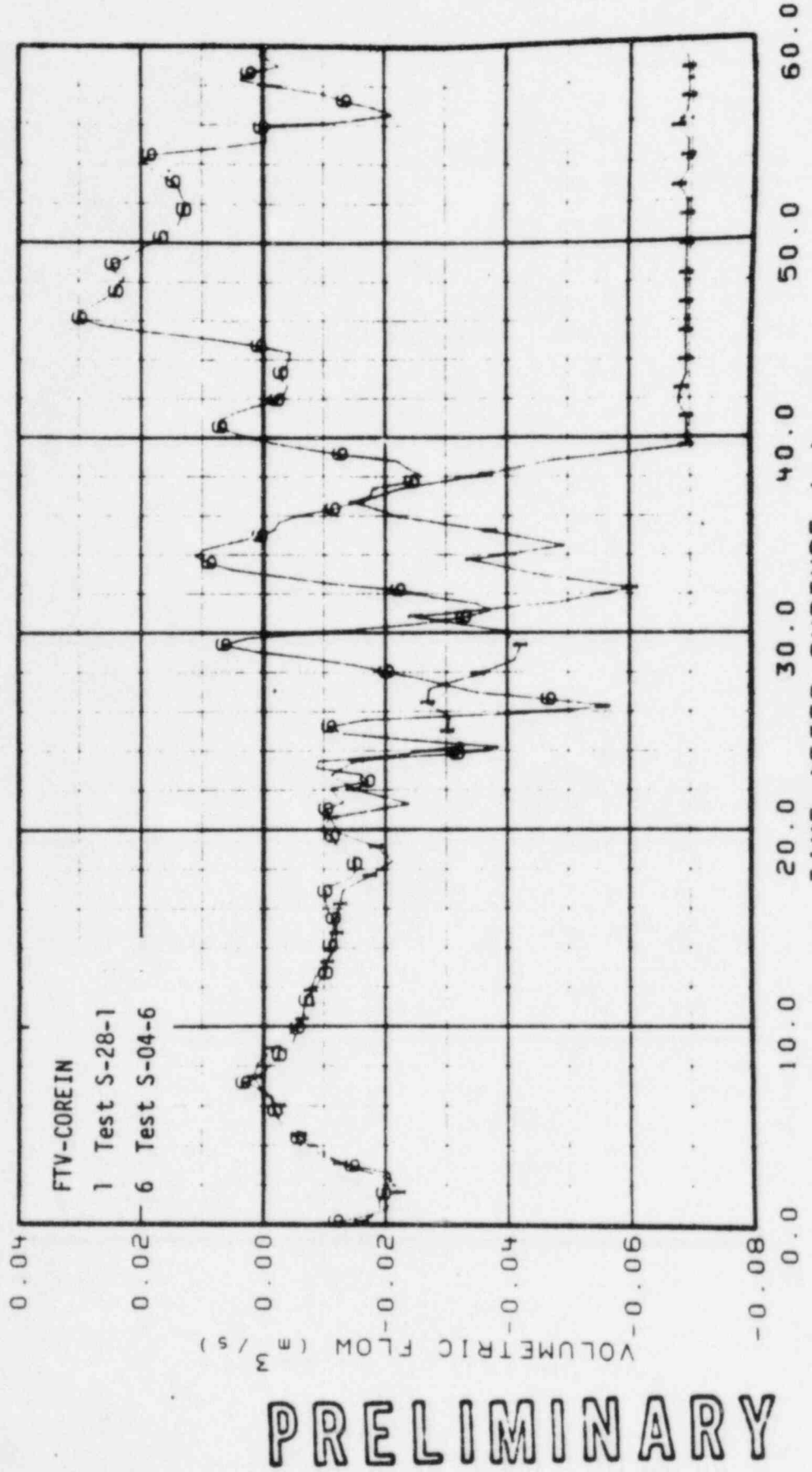

Figure 8. Comparison of Core Inlet Volumetric Flow - Short Term - Tests S-28-1 and S-04-6

PRELIMINARY

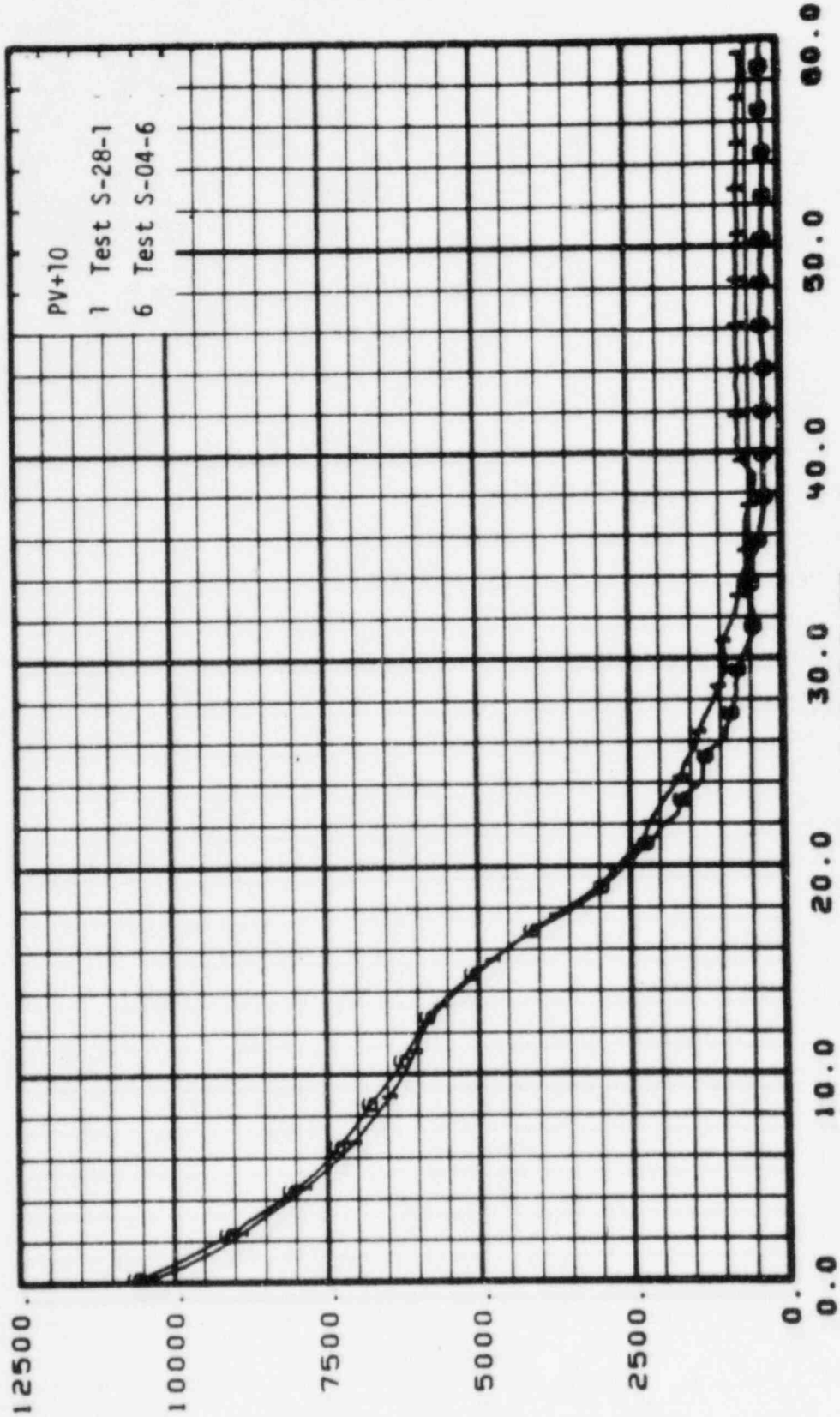

PRELIMINARY

Figure 9. Comparison of System Pressure - .Tests S-28-1 and S-04-6

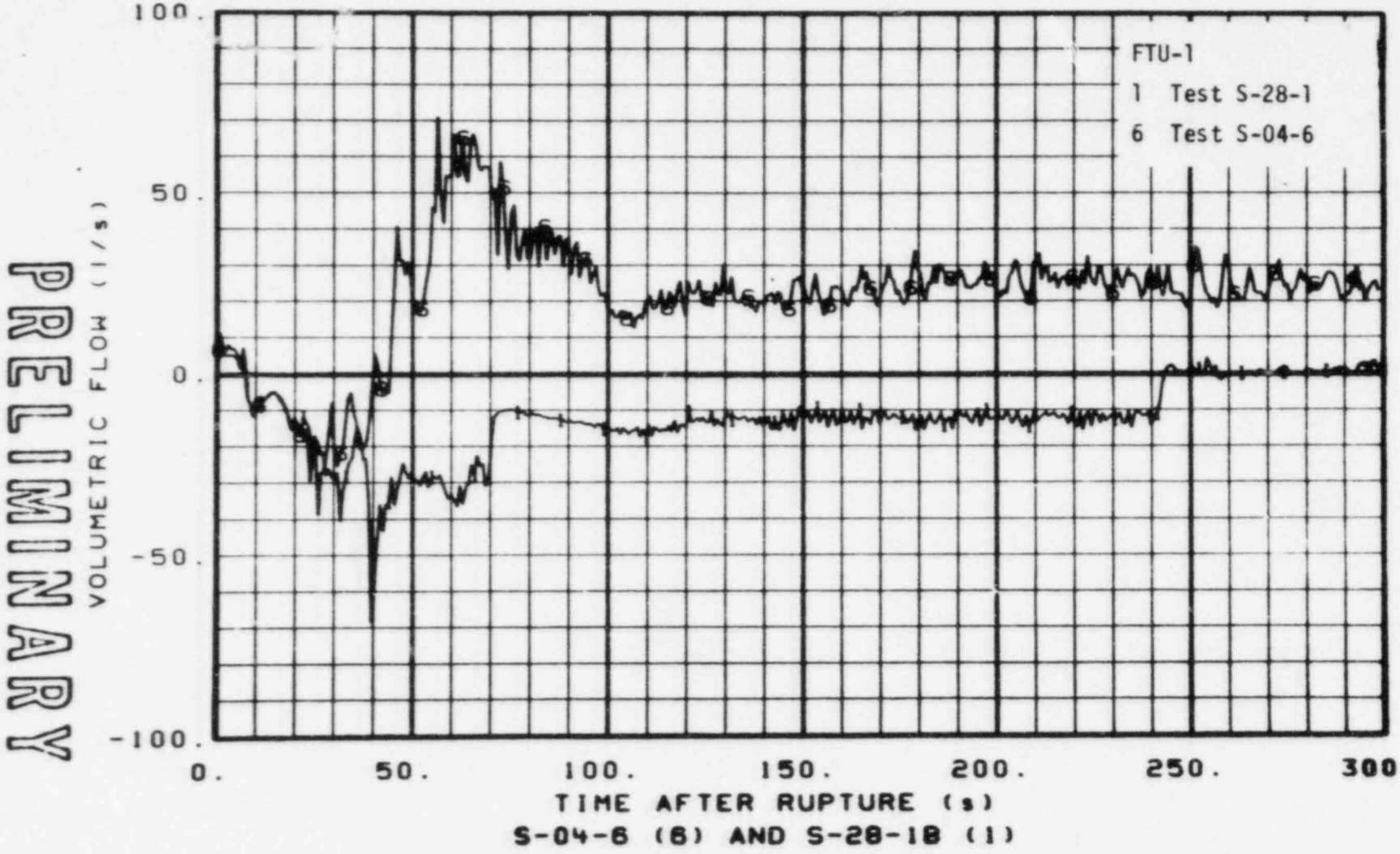

Figure 10. Comparison of Intact Loop Hot Leg Volumetric Flow Near the Vessel - Tests S-28-1 and S-04-6

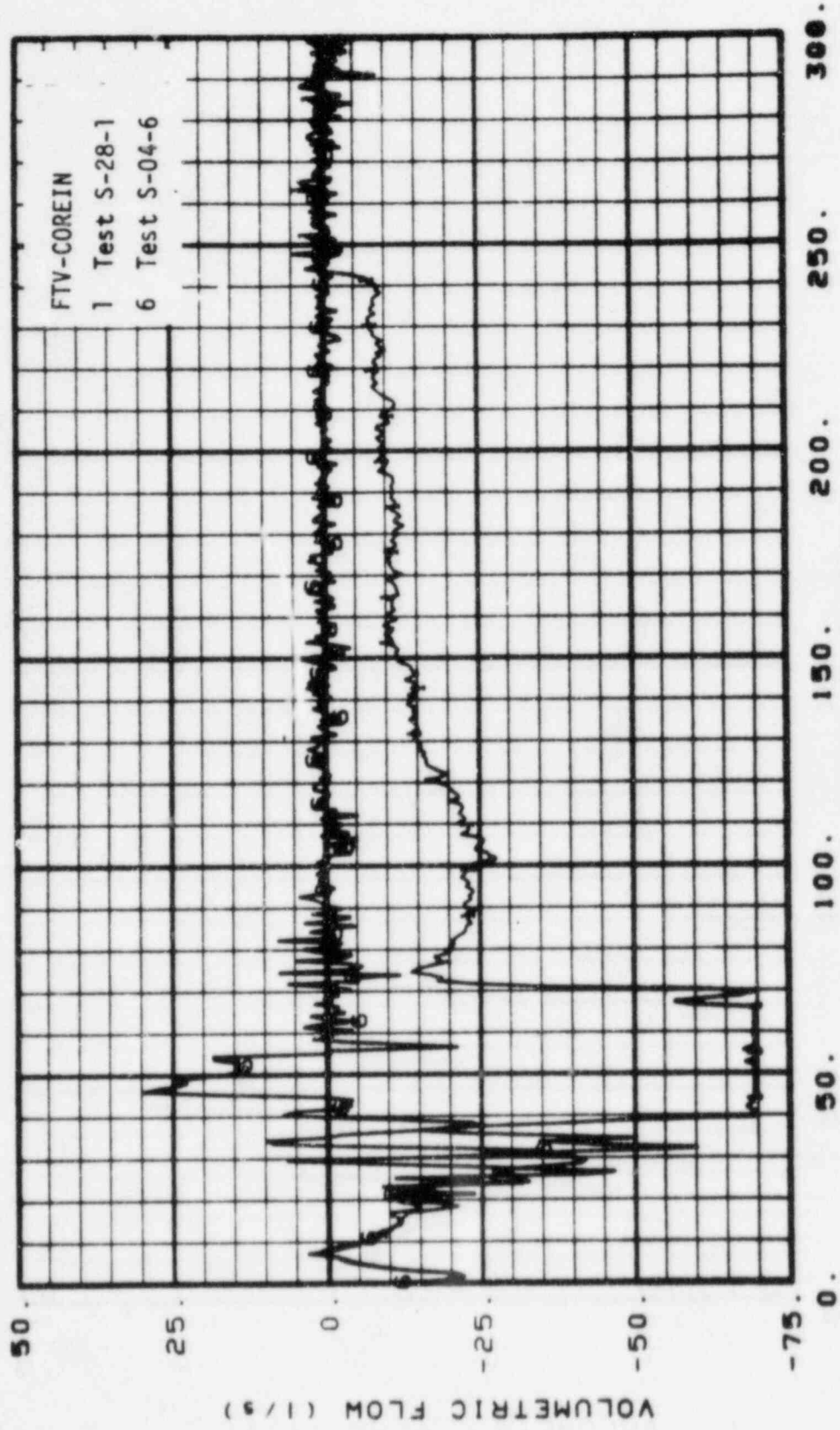

Figure 11. Comparison of Core Inlet Volumetric Flow - Long Term - Tests S-28-1 and S-04-6

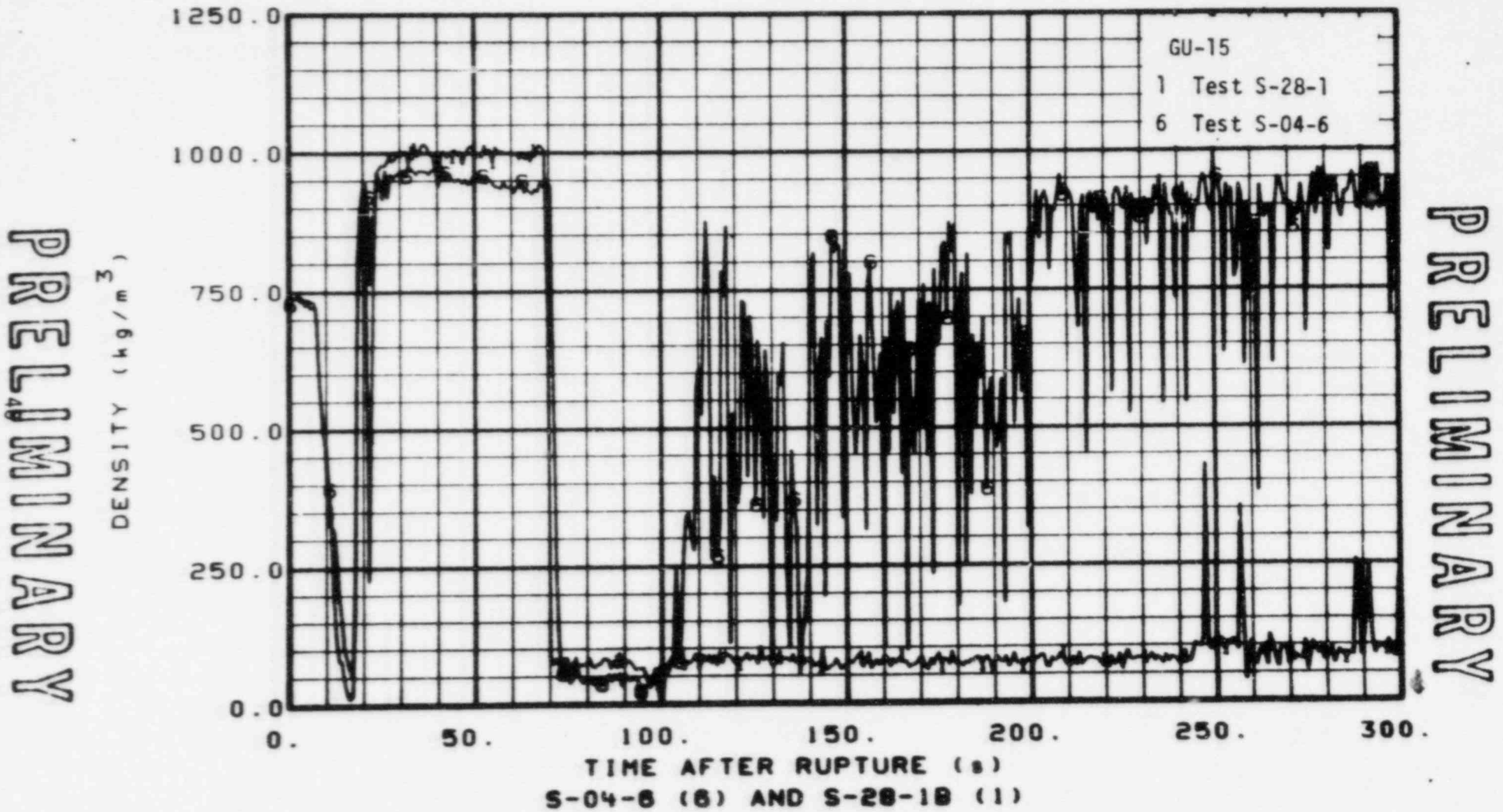

Figure 12. Comparison of Intact Loop Cold Leg Fluid Density Near the Vessel - Tests S-28-1 and S-04-6

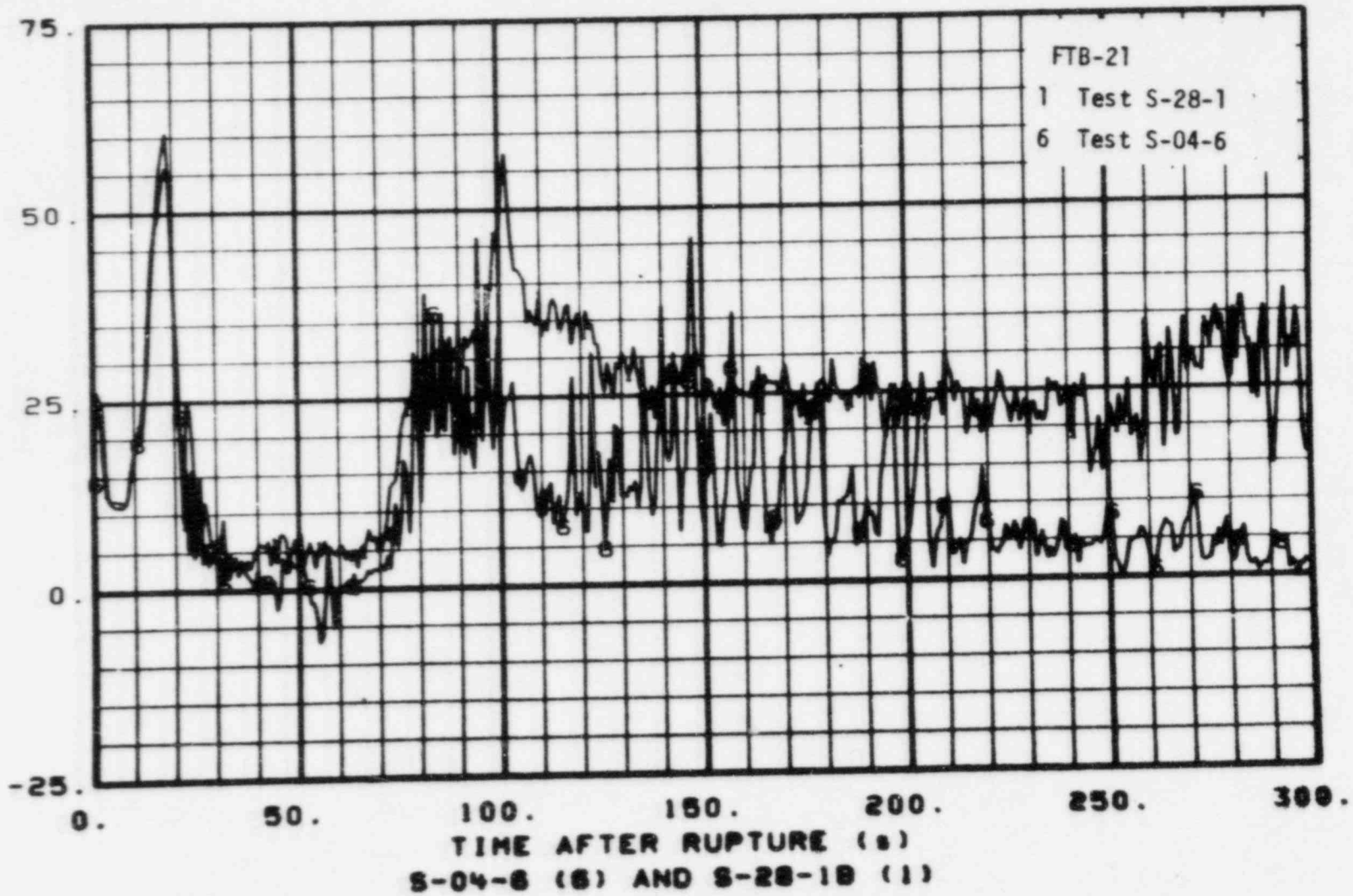

Figure 13. Comparison of Broken Loop Vessel Inlet Side Volumetric Flow - Tests S-28-1 and S-04-6

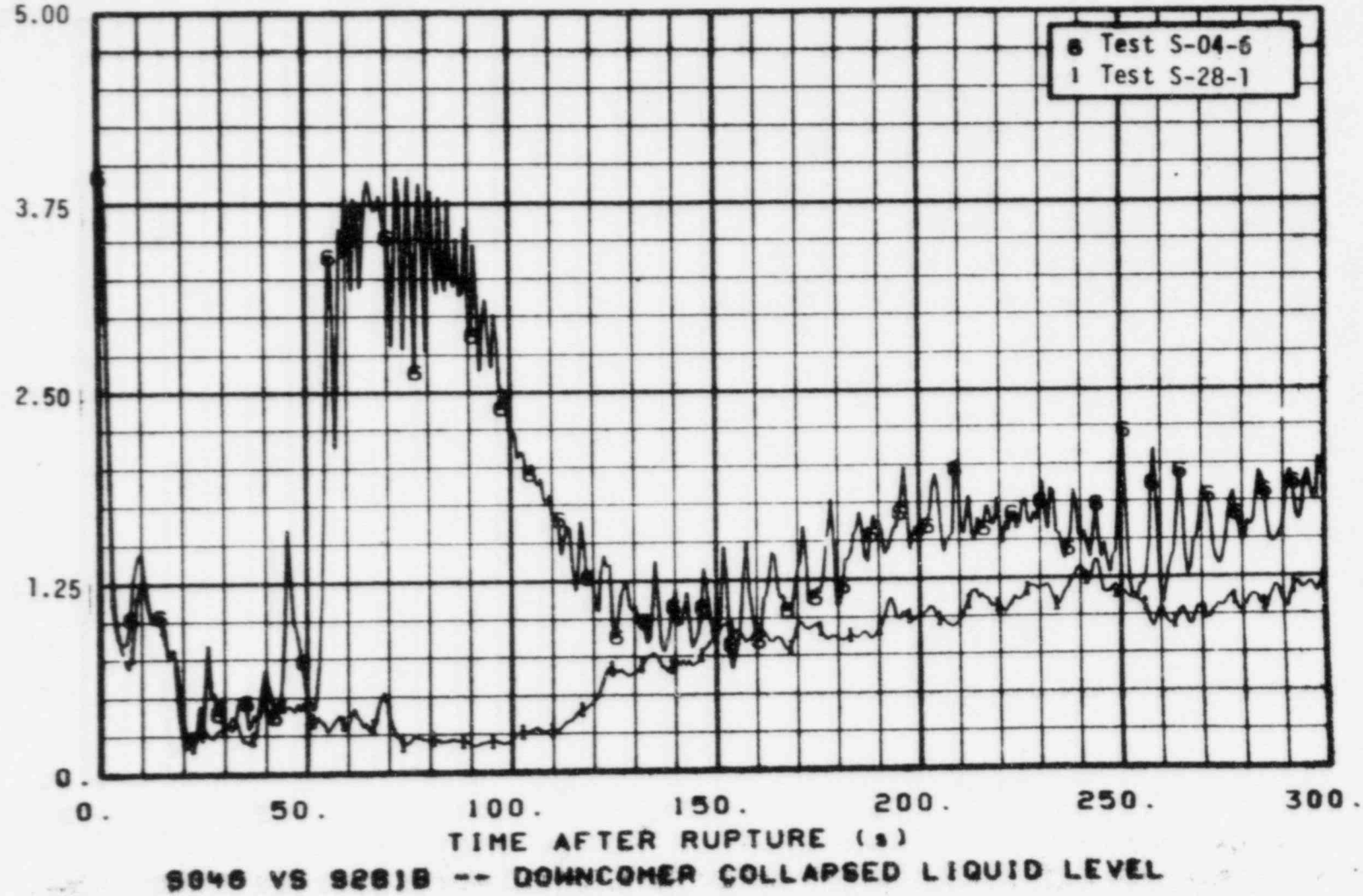

Figure 14. Comparison of Downcomer Collapsed Liquid Level - Tests S-28-1 and S-04-6

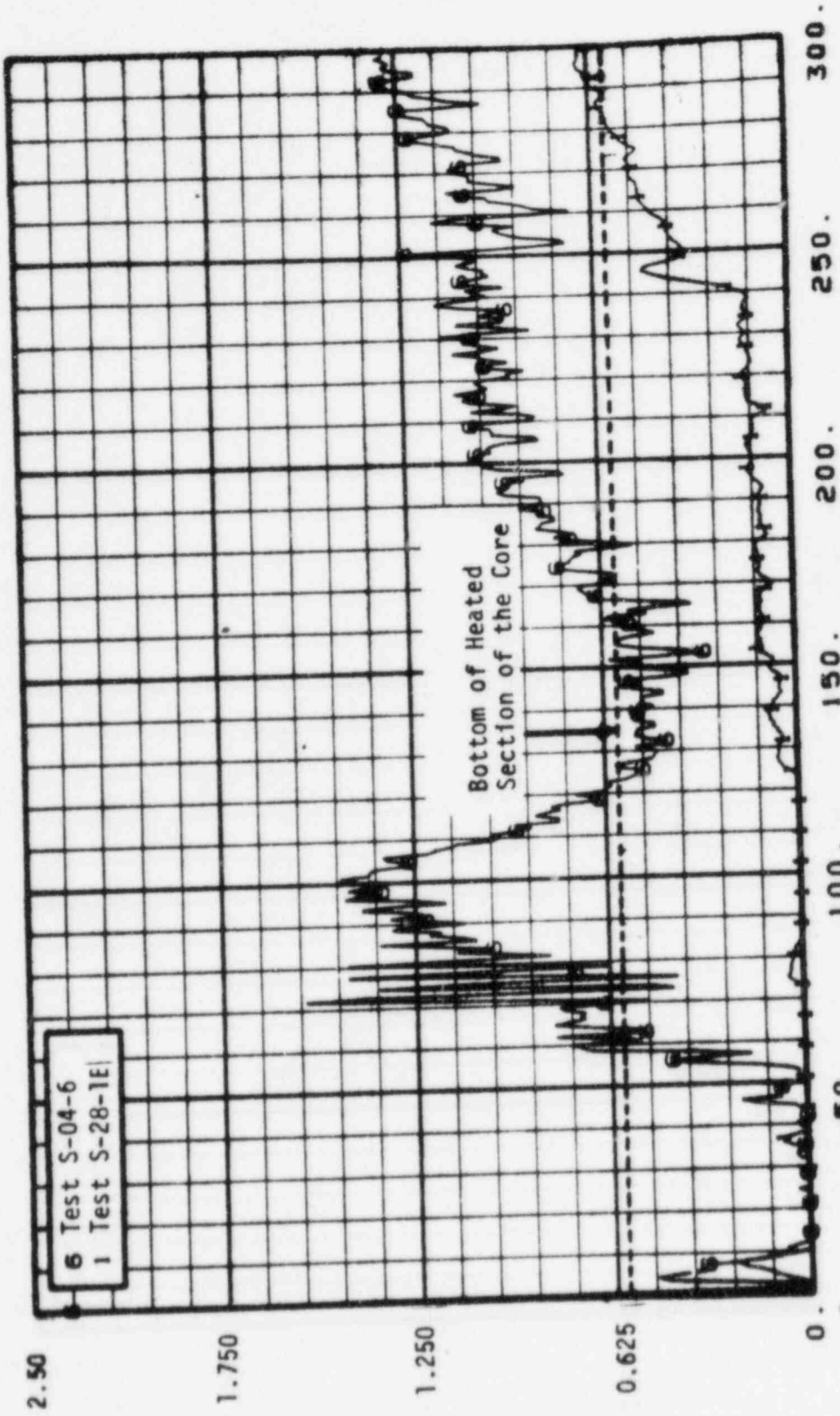

Figure 15. Comparison of Core Collapsed Liquid Level - Tests S-28-1 and S-04-6

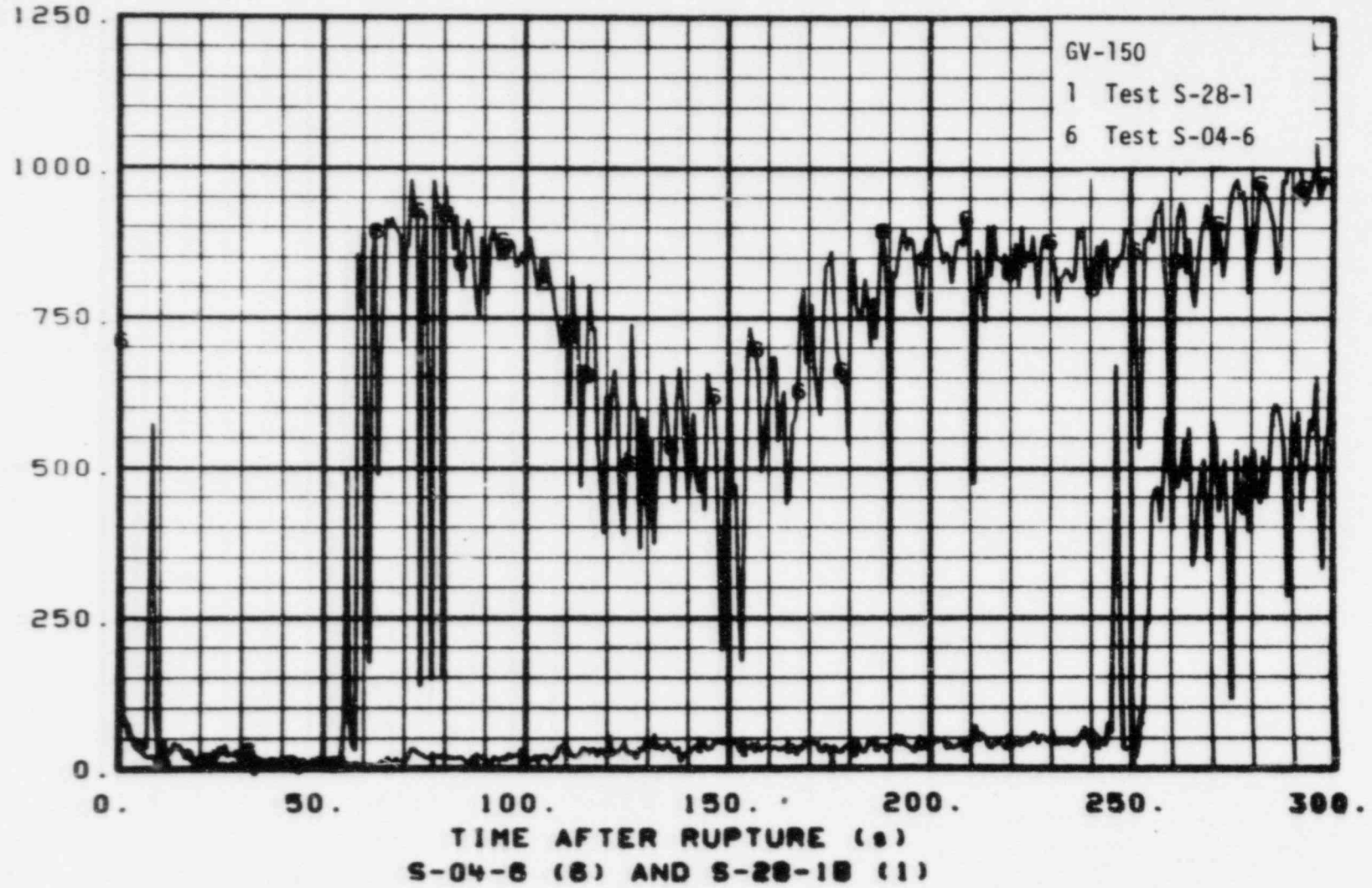

PRELIMINARY

PRELIMINARY

Figure 16. Comparison of Core Inlet Fluid Density - Tests S-28-1 and S-04-6

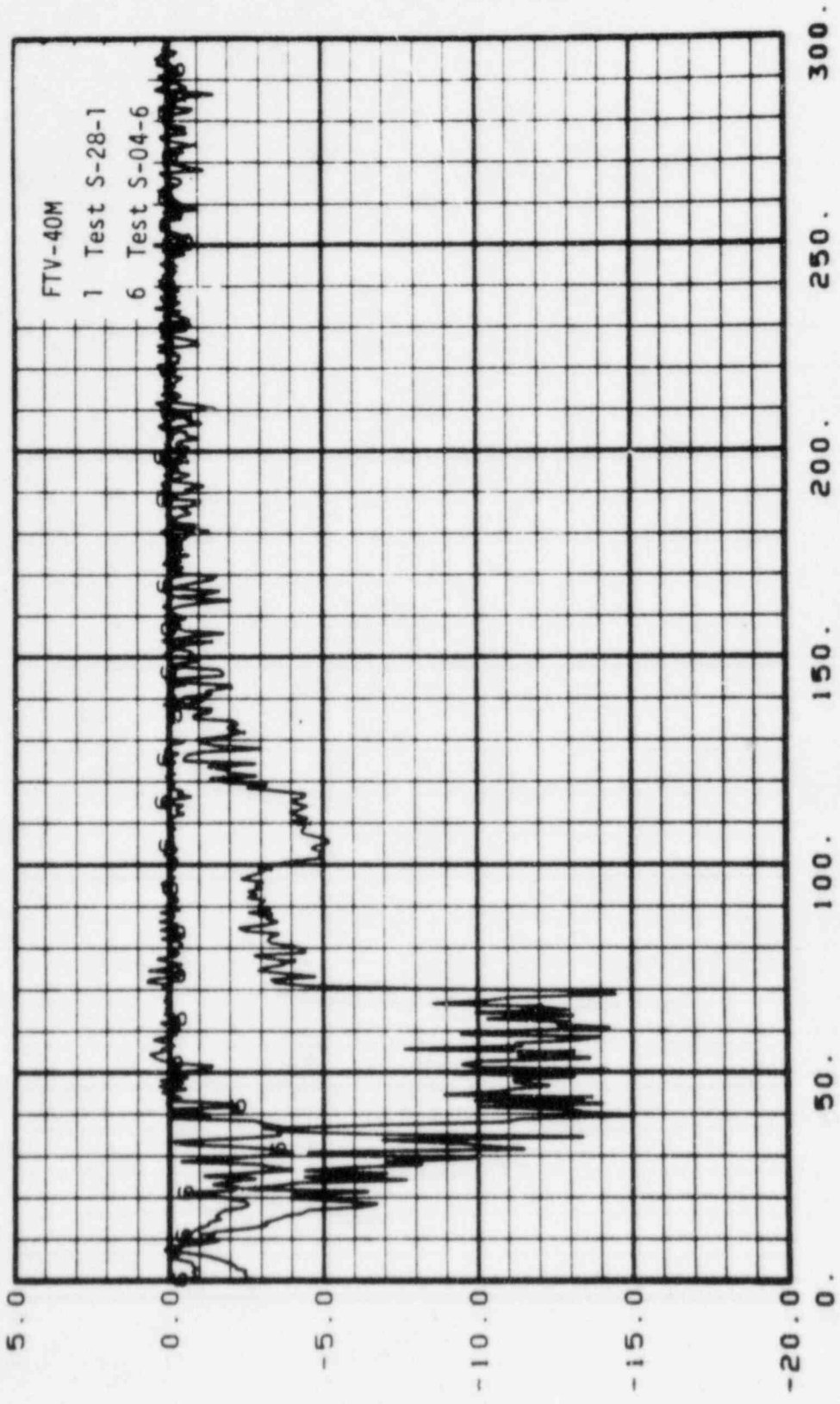

Figure 17. Comparison of Downcomer Fluid Velocity - Tests S-28-1 and S-04-6

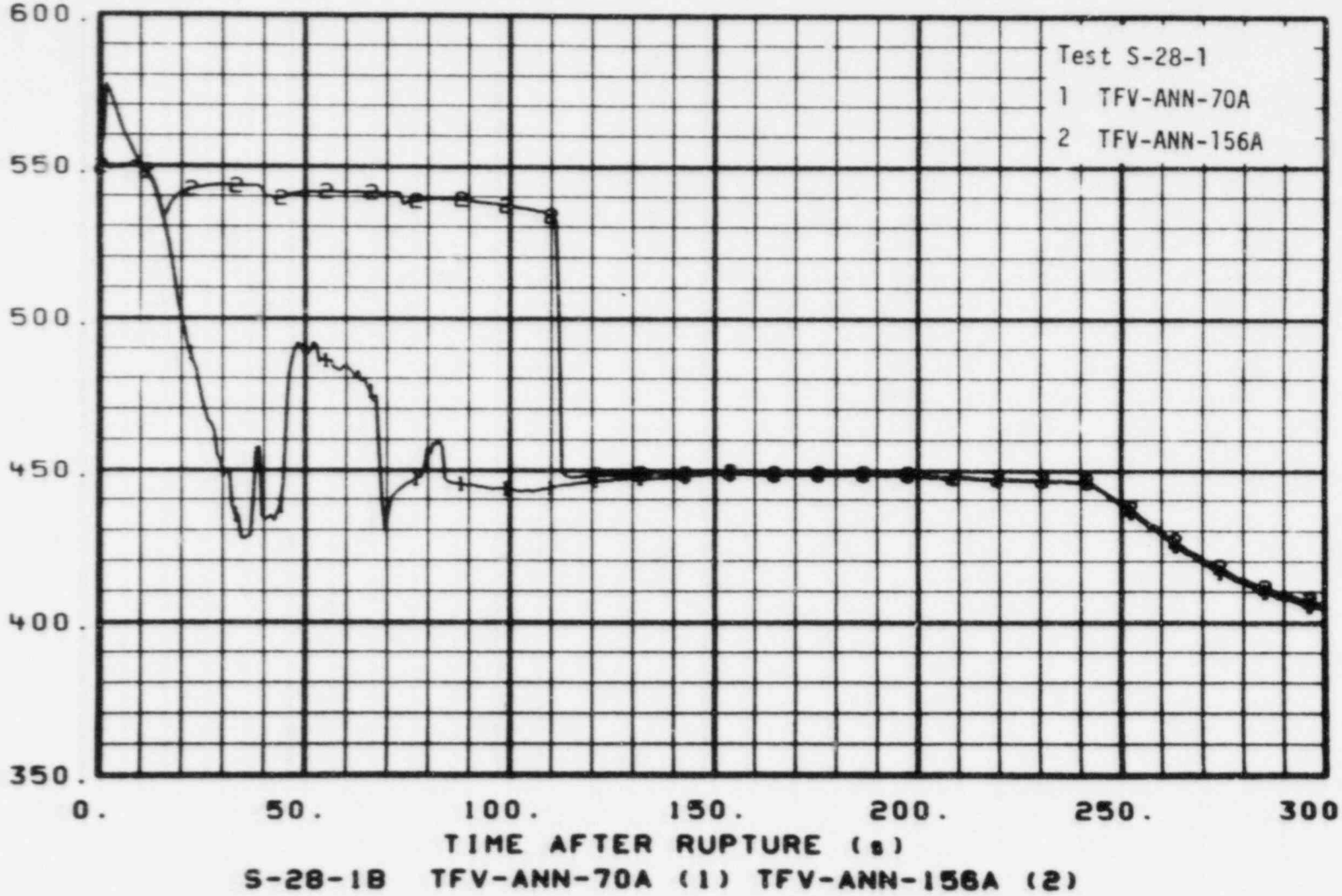

Figure 18. Comparison of Downcomer Fluid Temperatures - Test S-28-1

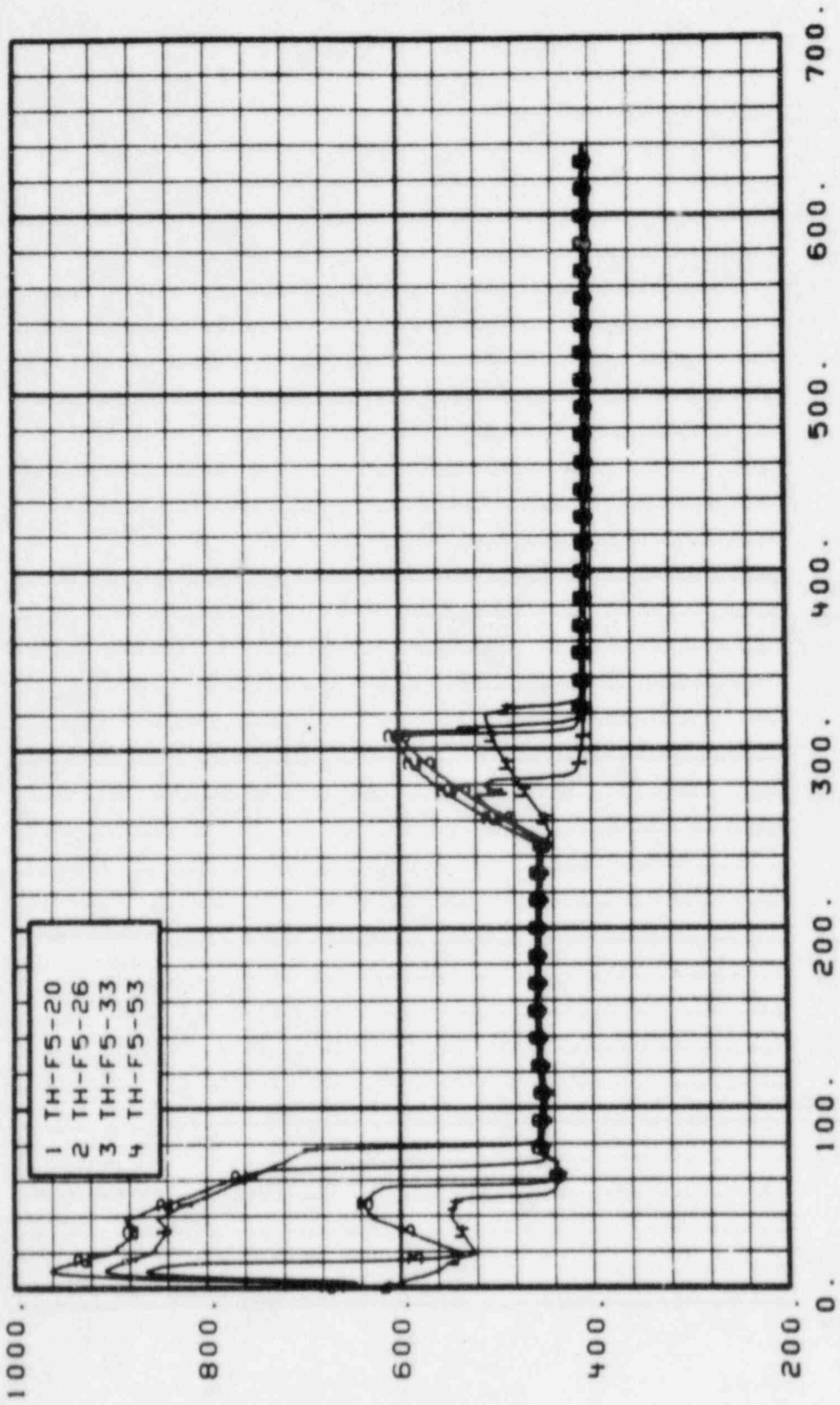

Figure 19. Cladding Temperatures on Rod F5 - Test S-28-1

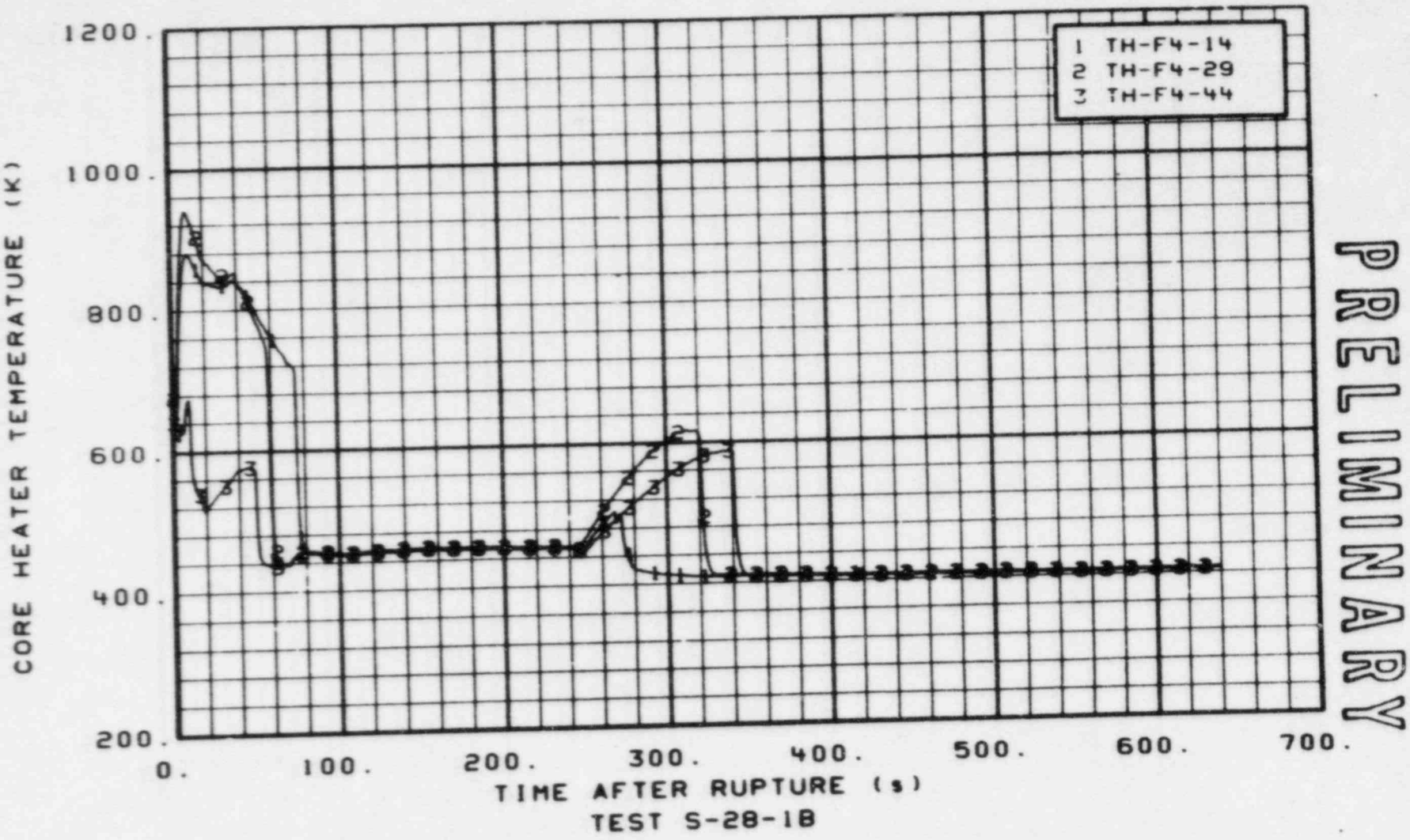

PRELIMINARY

Figure 20. Cladding Temperatures on Rod F4 - Test S-28-1

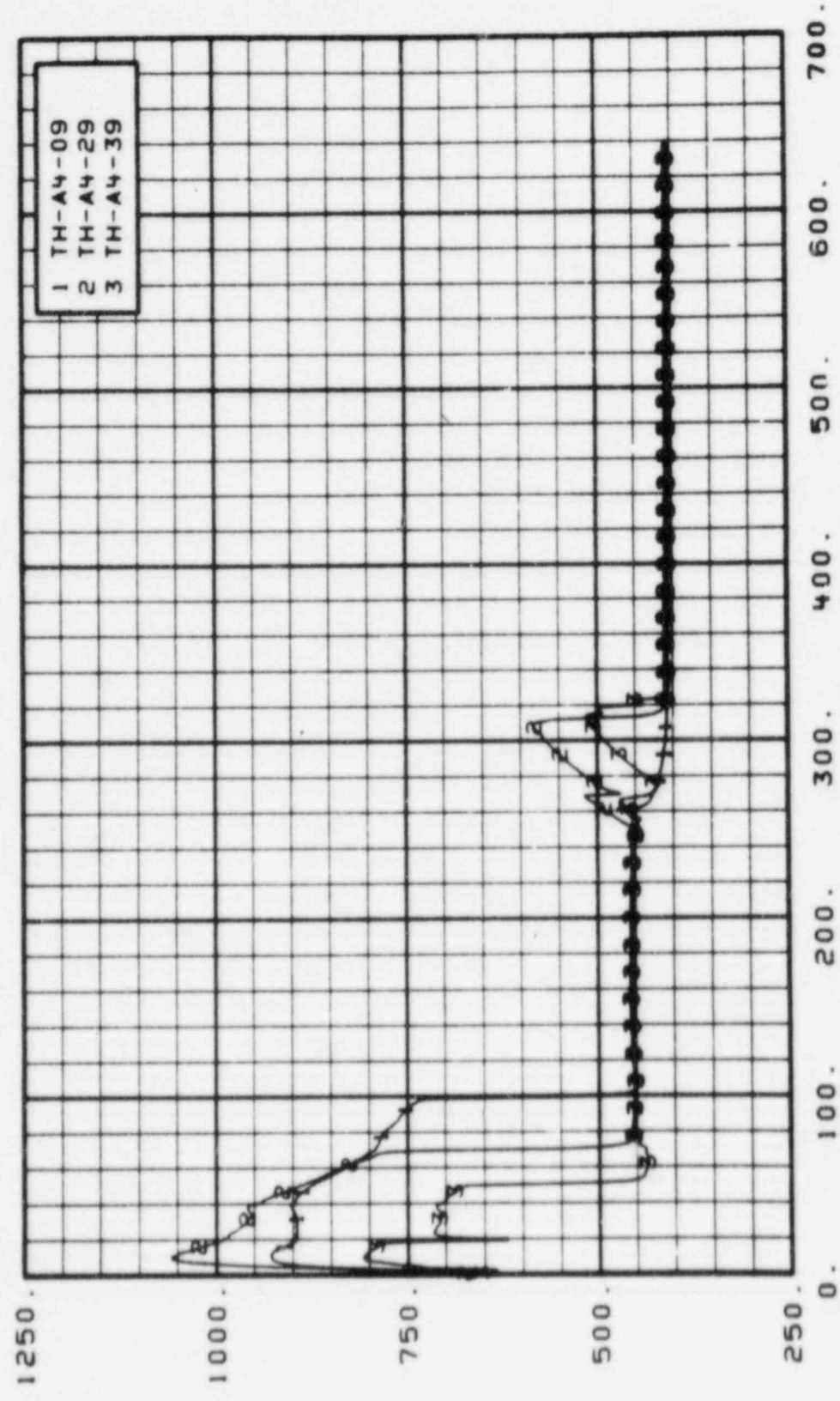

Figure 21. Cladding Temperatures on Rod A4 - Test S-28-1

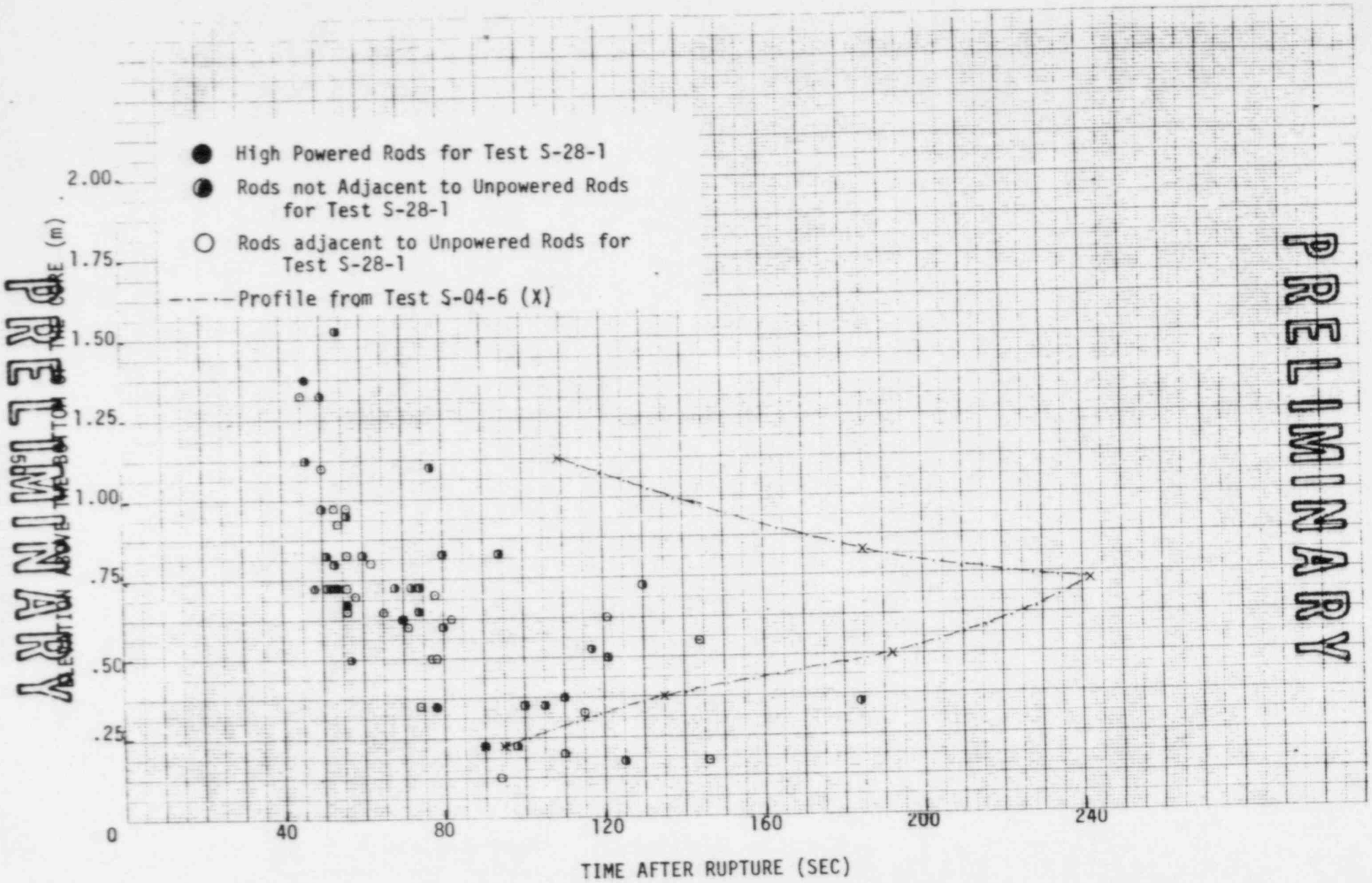

Figure 22. Rod Quench Times Versus Elevation - Test S-28-1

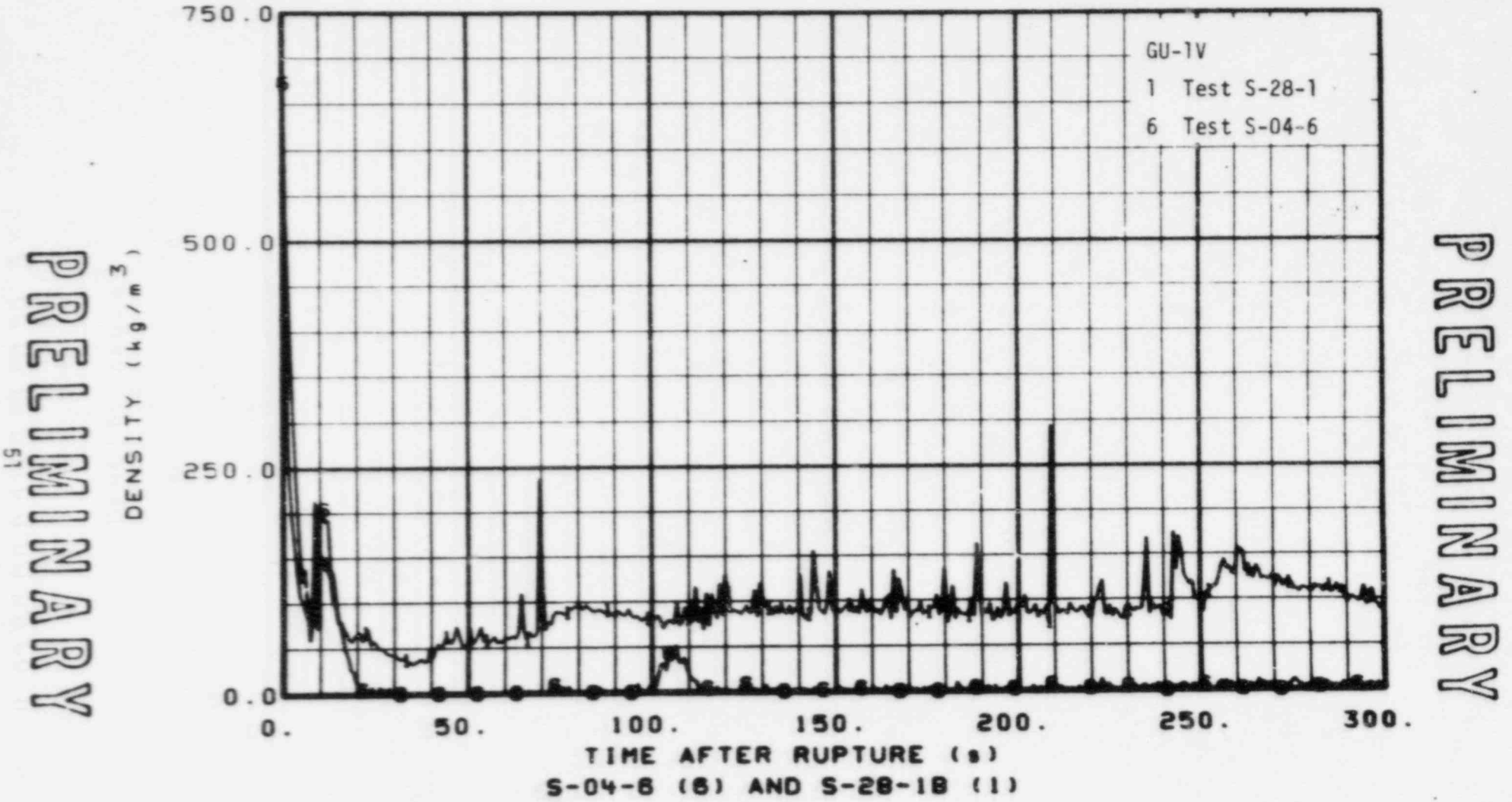

Figure 23. Comparison of Intact Loop Hot Leg Fluid Density Near Vessel - Tests S-28-1 and S-04-6

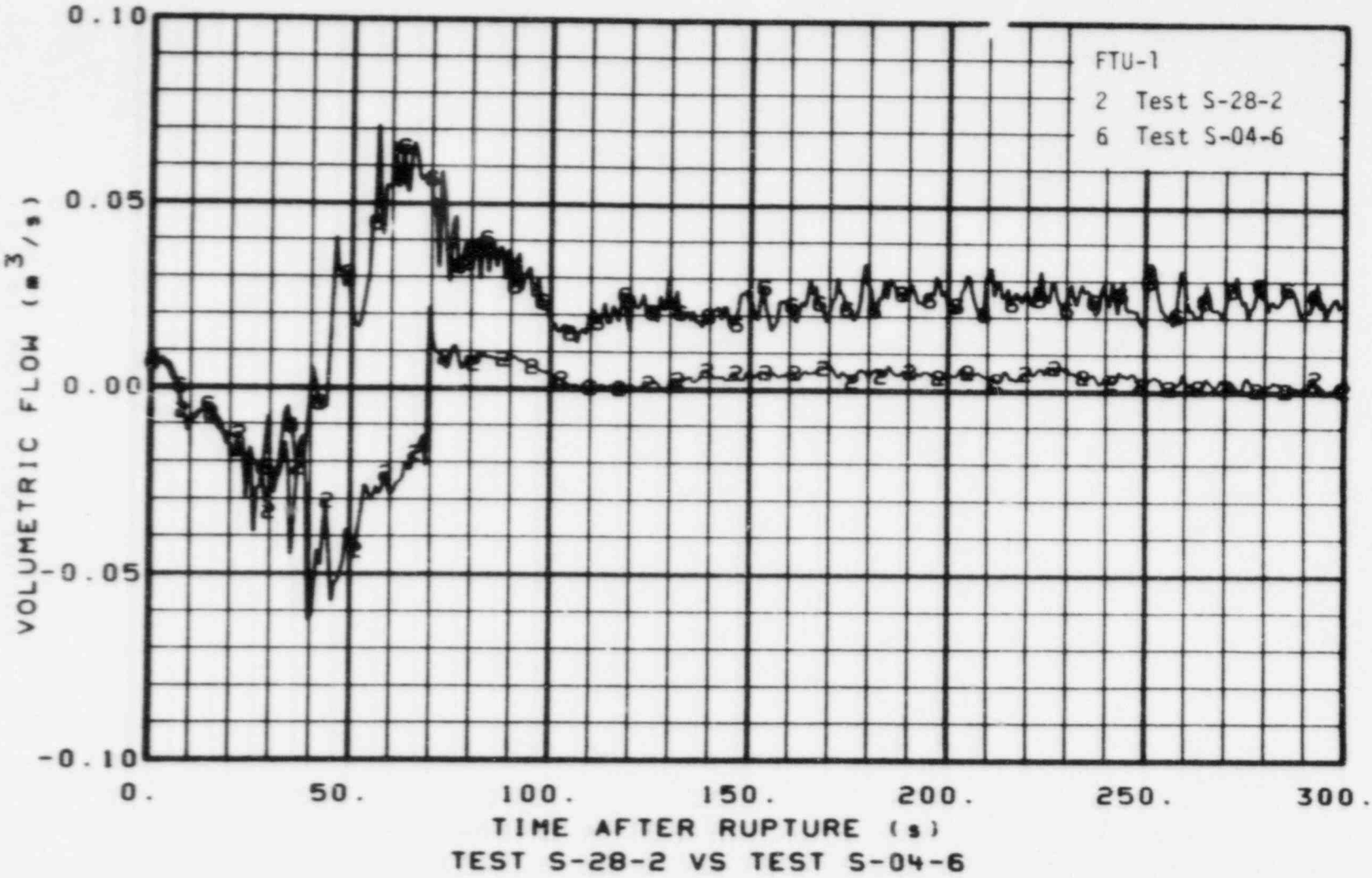

Figure 24. Comparison of Intact Loop Hot Leg Volumetric Flow Near Vessel - Tests S-28-2 and S-04-6

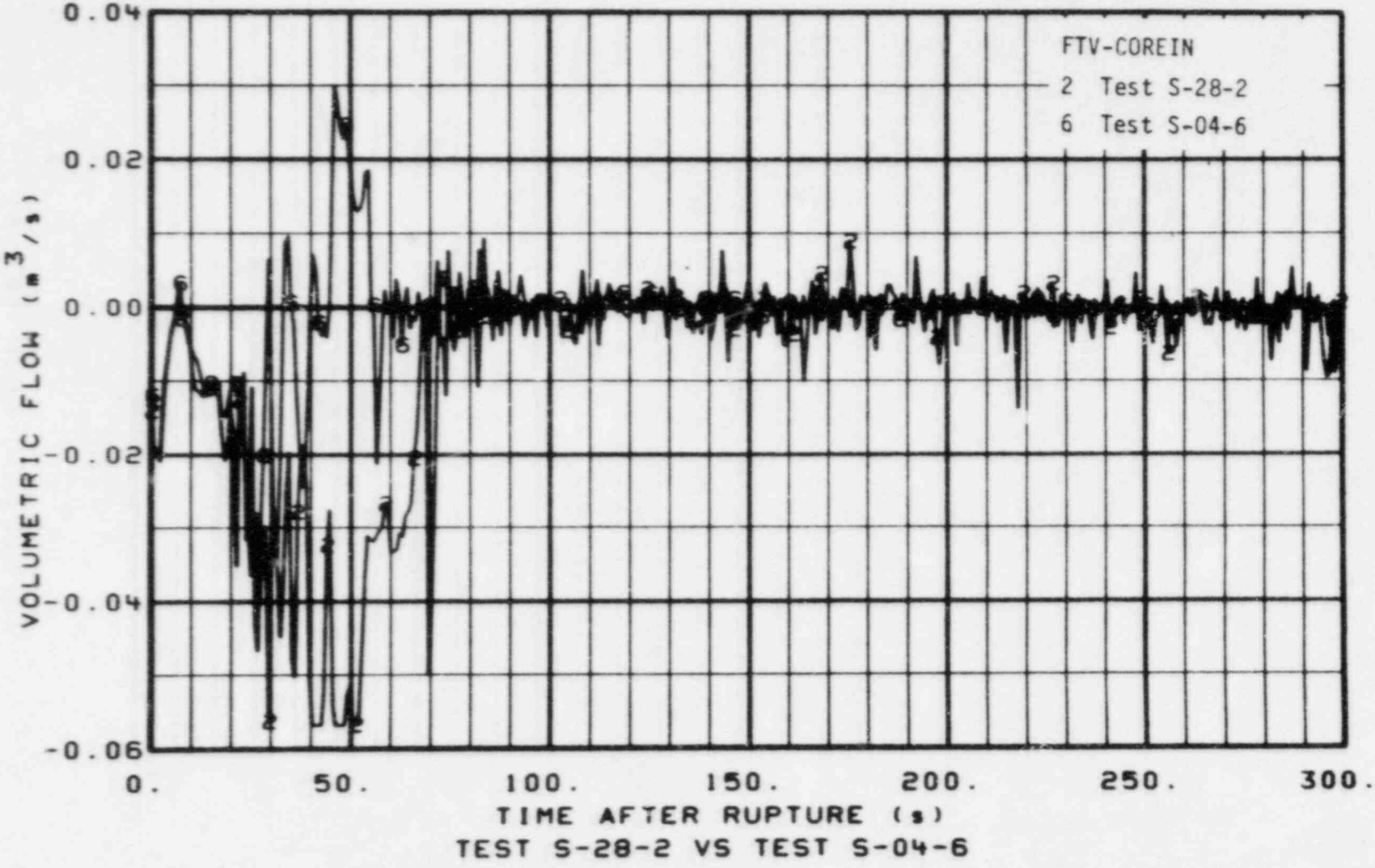

PRELIMINARY

Figure 25. Comparison of Core Inlet Volumetric Flow - Tests S-28-2 and S-04-6

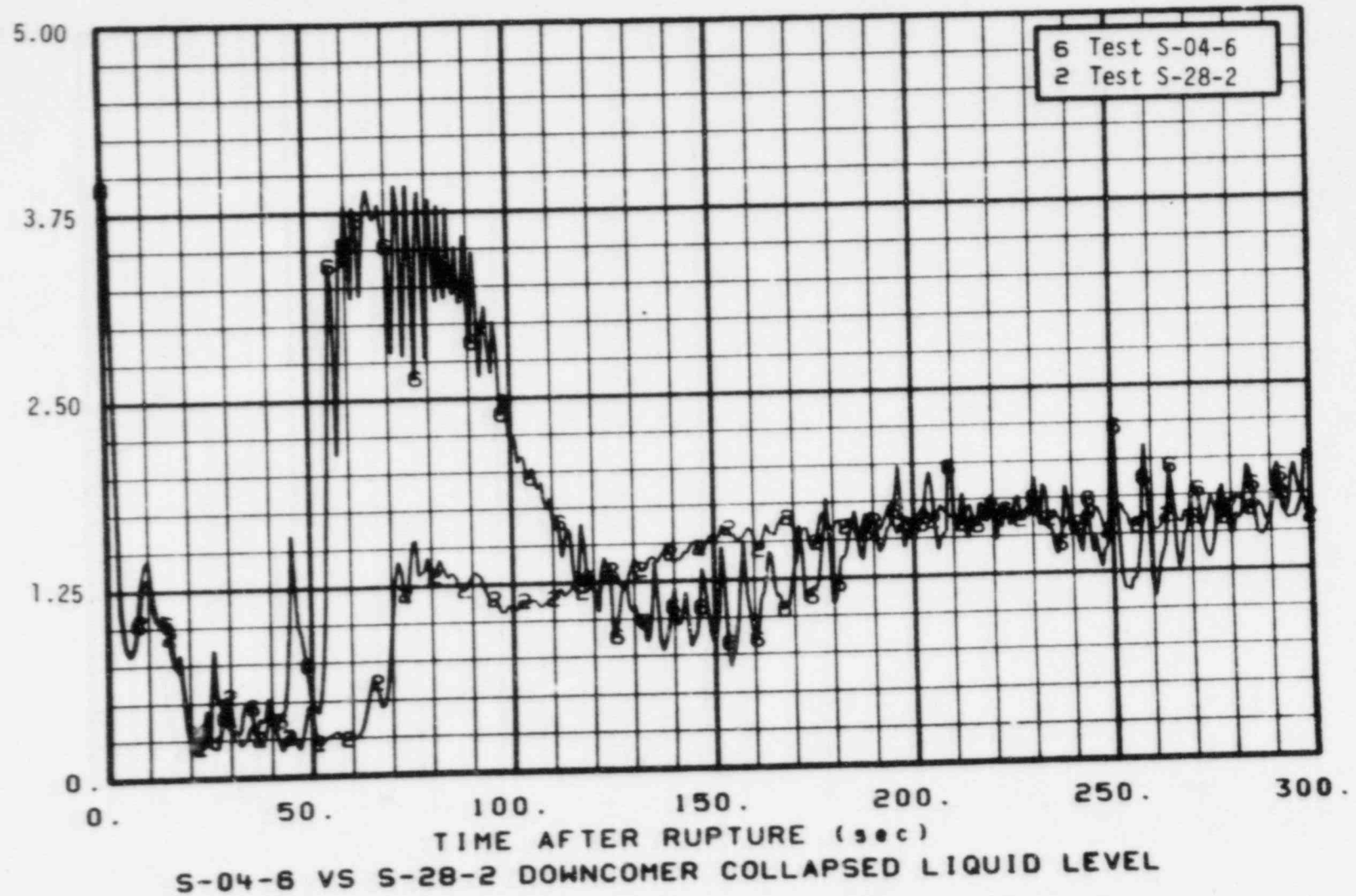

PRELIMINARY

Figure 26. Comparison of Downcomer Collapsed Liquid Level - Tests S-28-2 and S-04-6

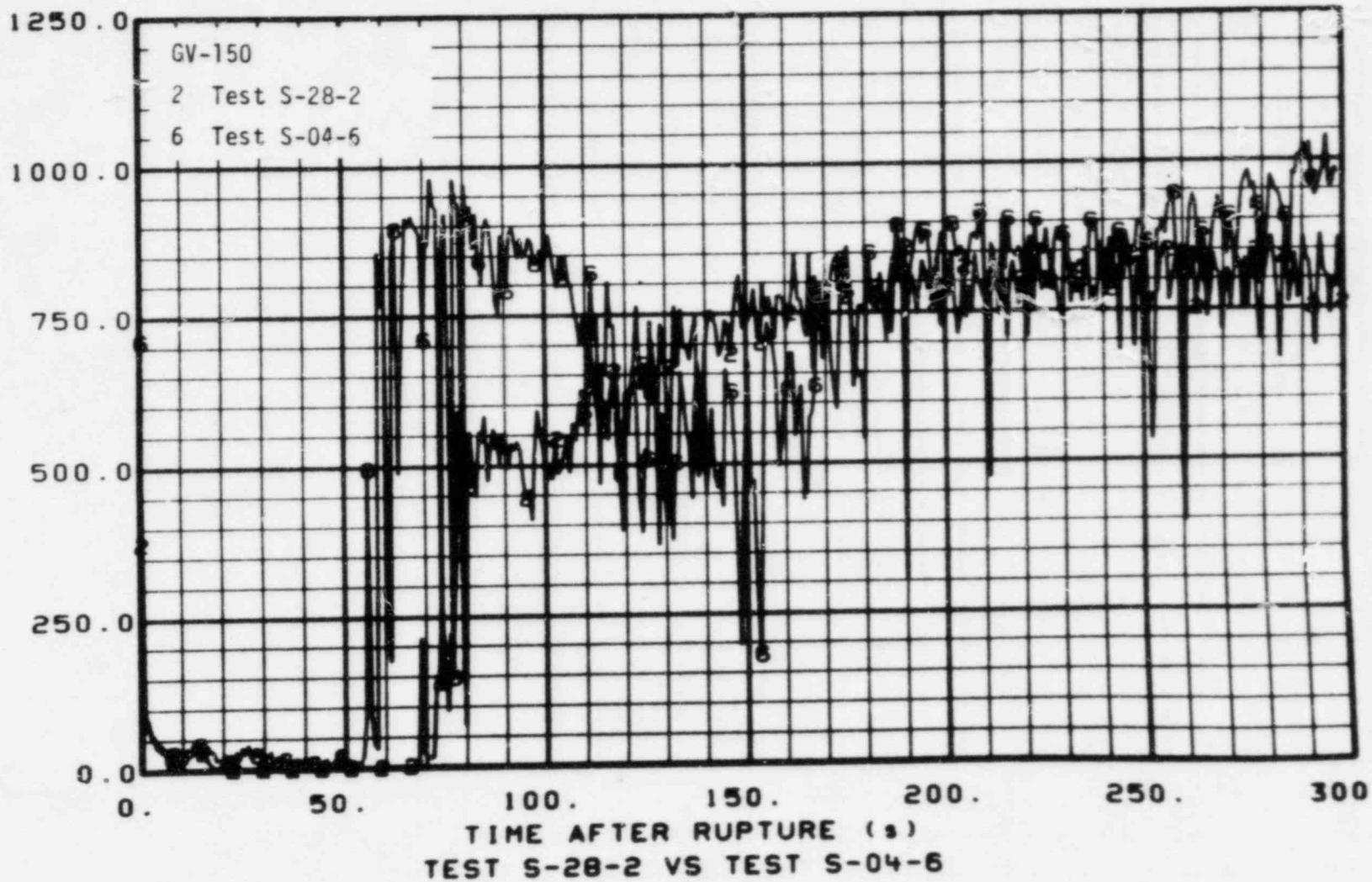

Figure 27. Comparison of Core Inlet Fluid Density - Tests S-28-2 and S-04-6

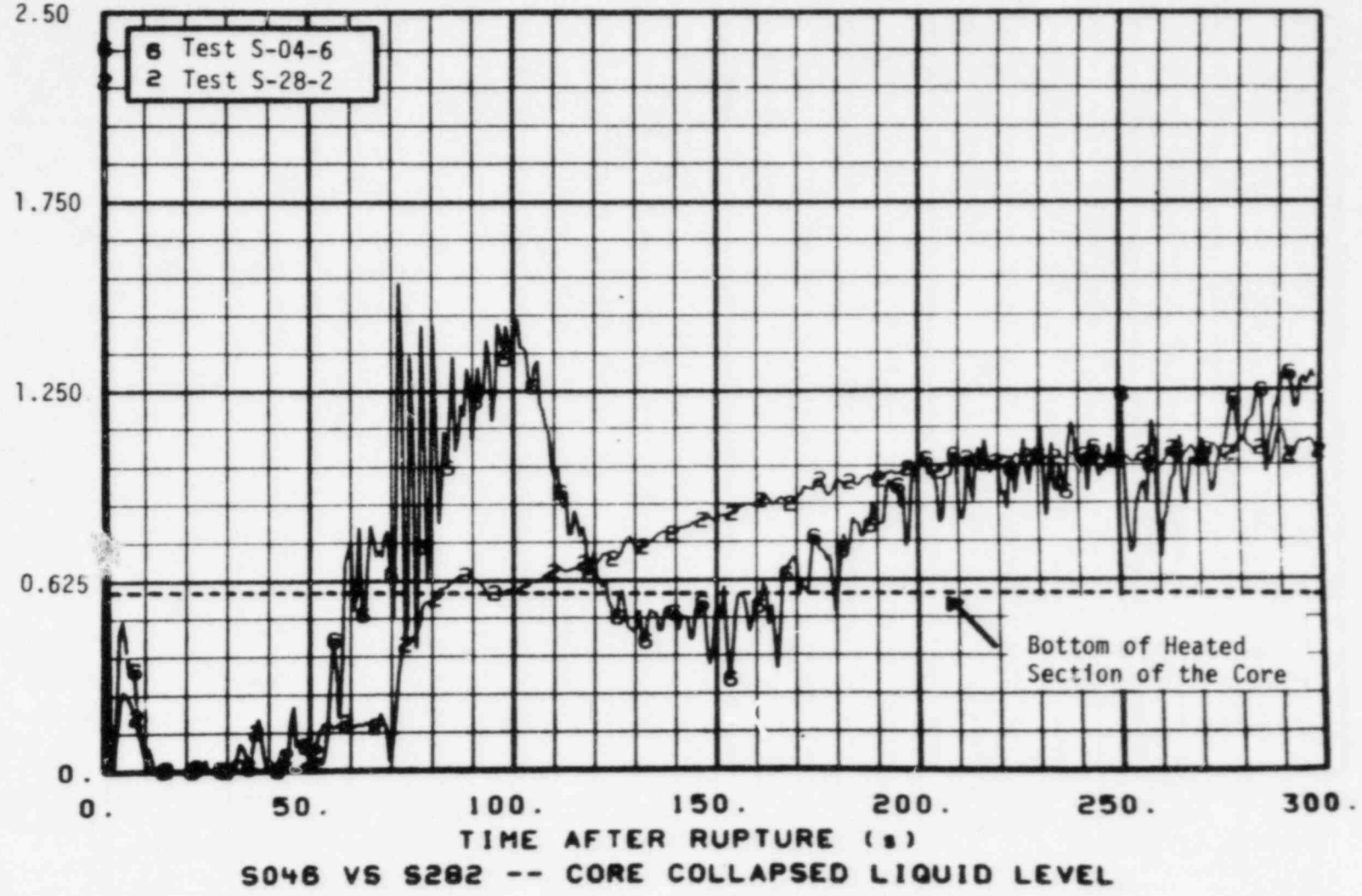

Figure 28. Comparison of Core Collapsed Liquid Level - Tests S-28-2 and S-04-6

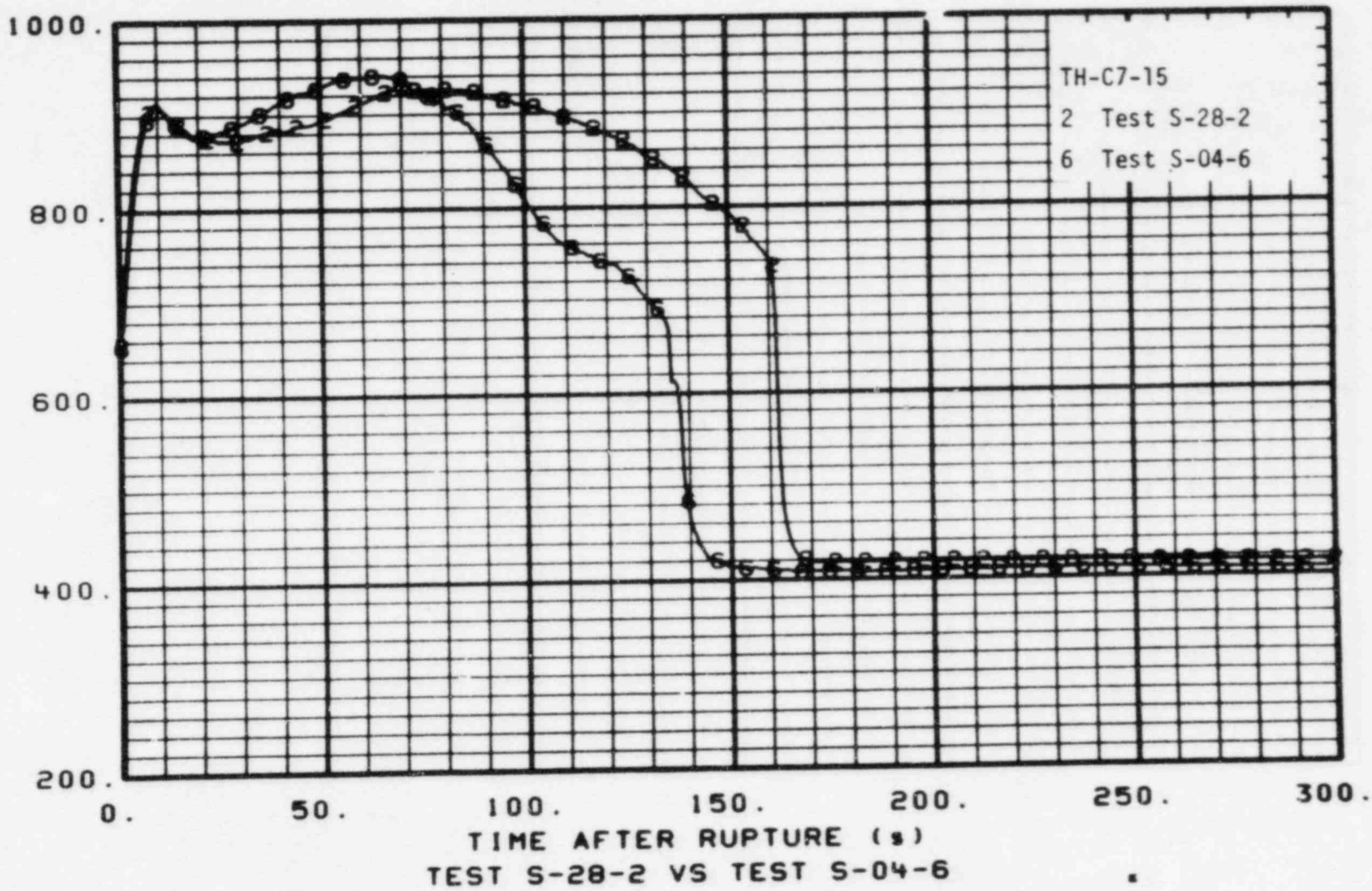

Figure 29. Comparison of Cladding Temperatures on Rod C7 at the 0.38 Meter Elevation - Tests S-28-2 and S-04-6

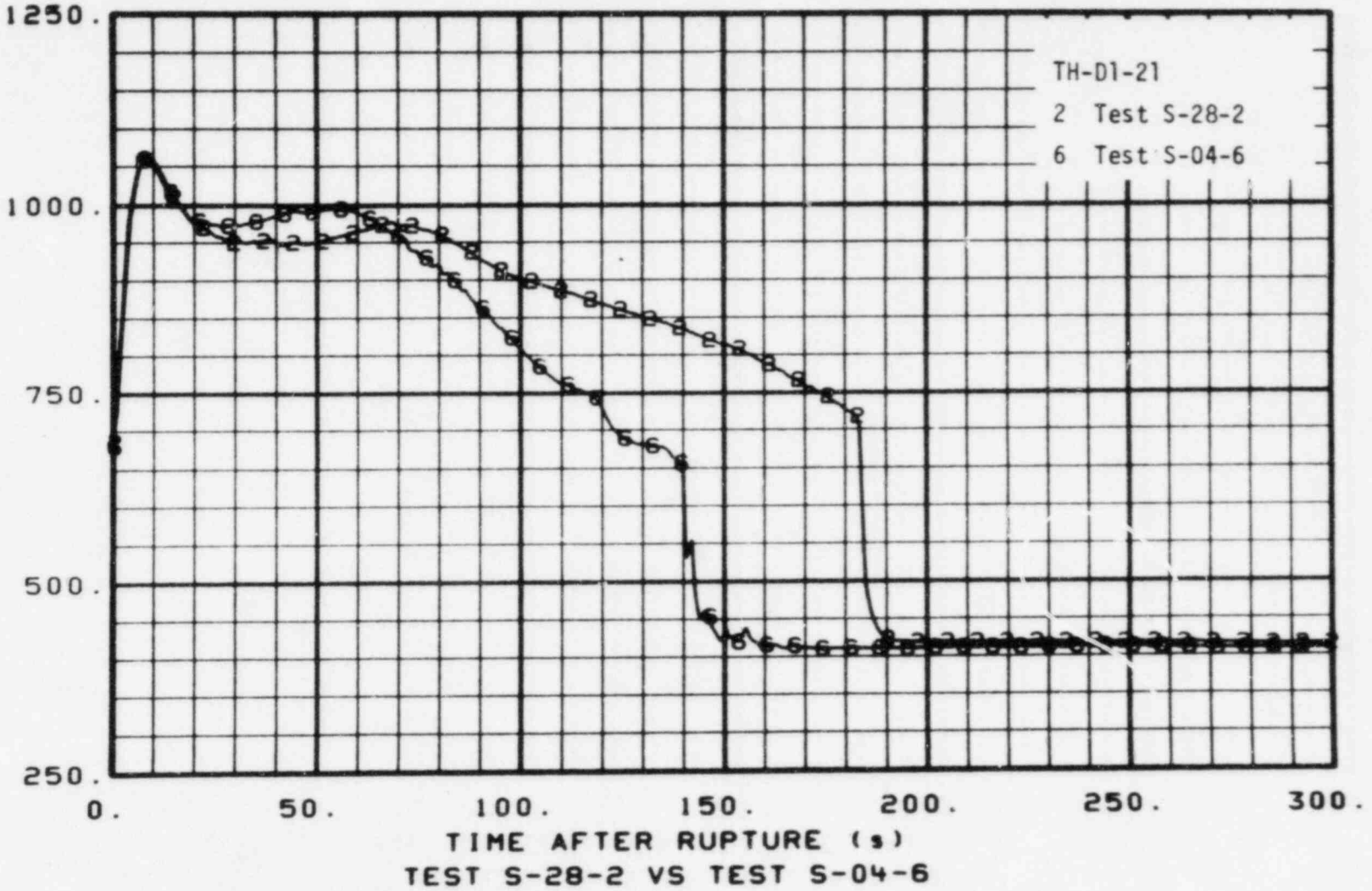

Figure 30. Comparison of Cladding Temperatures on Rod D1 at the 0.53 Meter Elevation - Tests S-28-2 and S-04-6

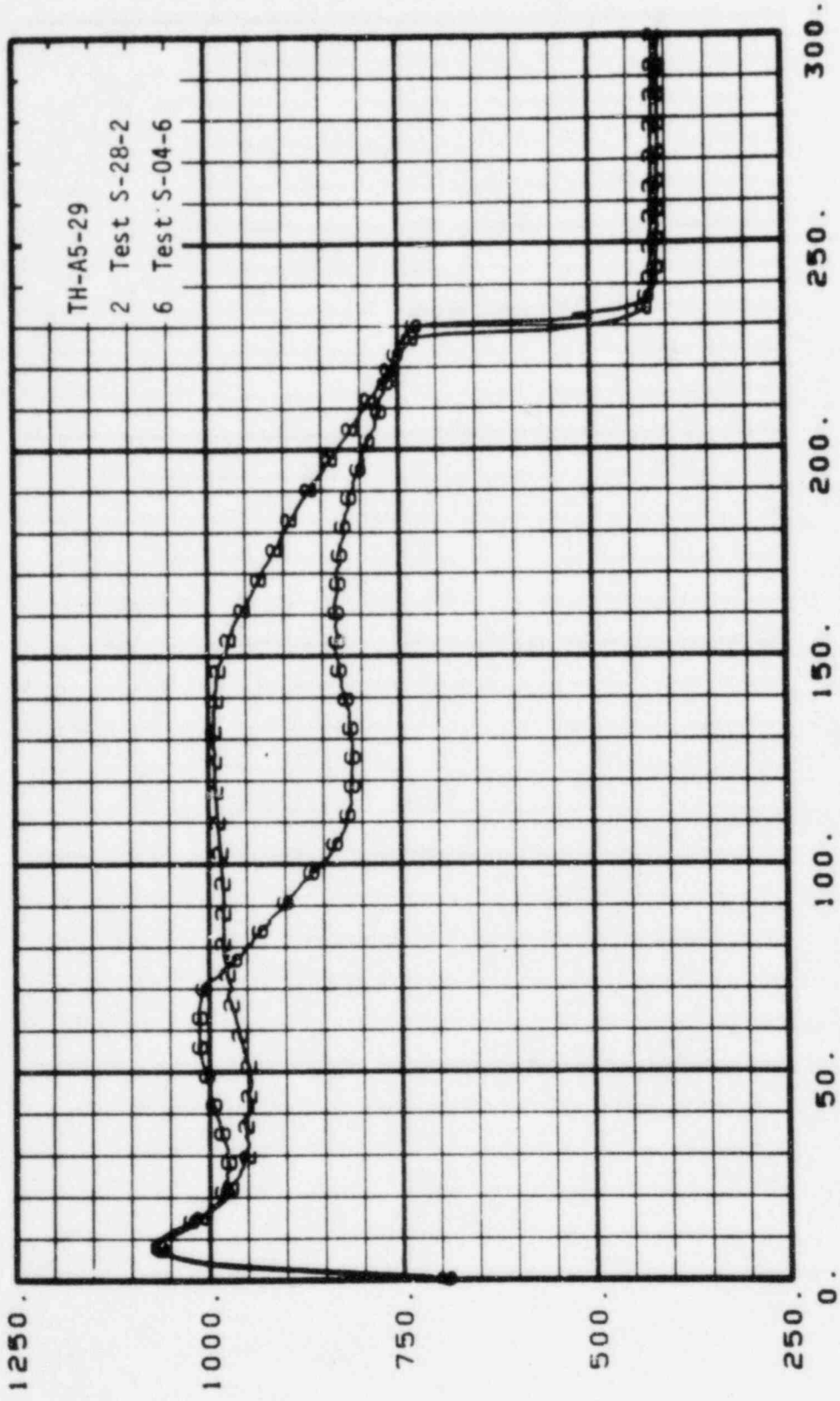

Figure 31. Comparison of Cladding Temperatures on Rod A5 at the 0.74 Meter Elevation - Tests S-28-2 and S-04-6

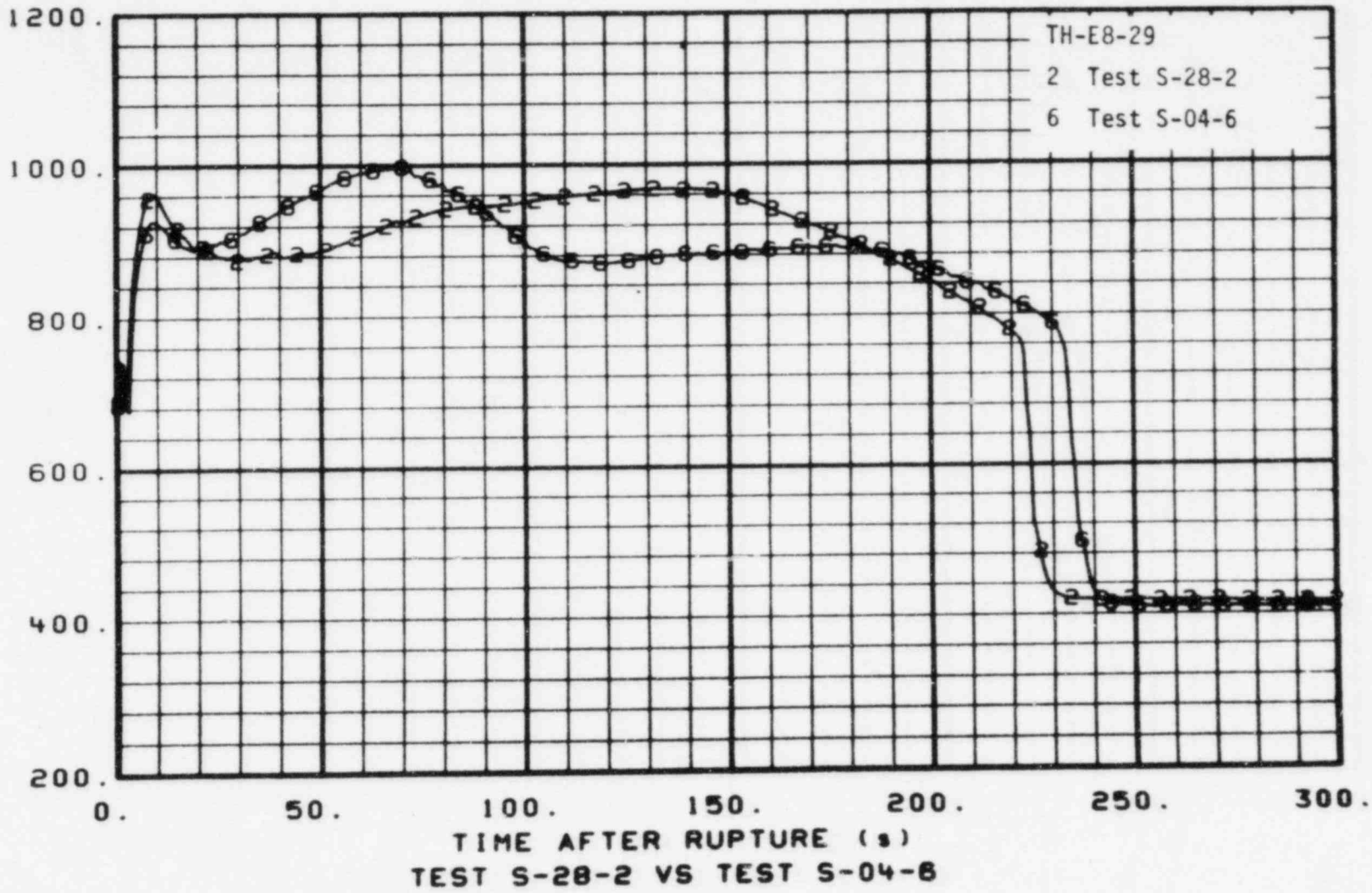

Figure 32. Comparison of Cladding Temperatures on Rod E8 at the 0.74 Meter Elevation - Tests S-28-2 and S-04-6

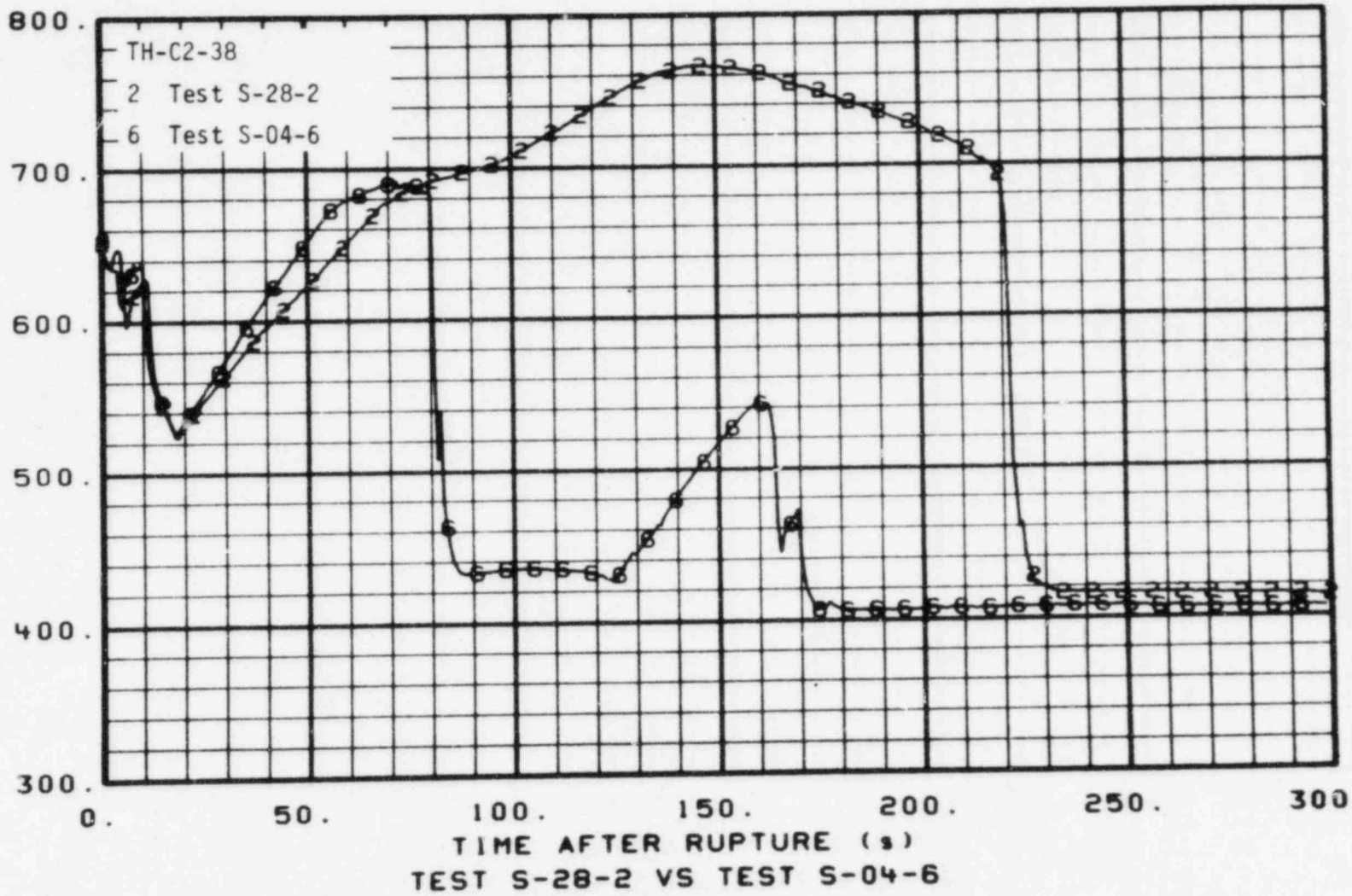

Figure 33. Comparison of Cladding Temperatures on Rod C2 at the 0.97 Meter Elevation - Tests S-28-2 and S-04-6

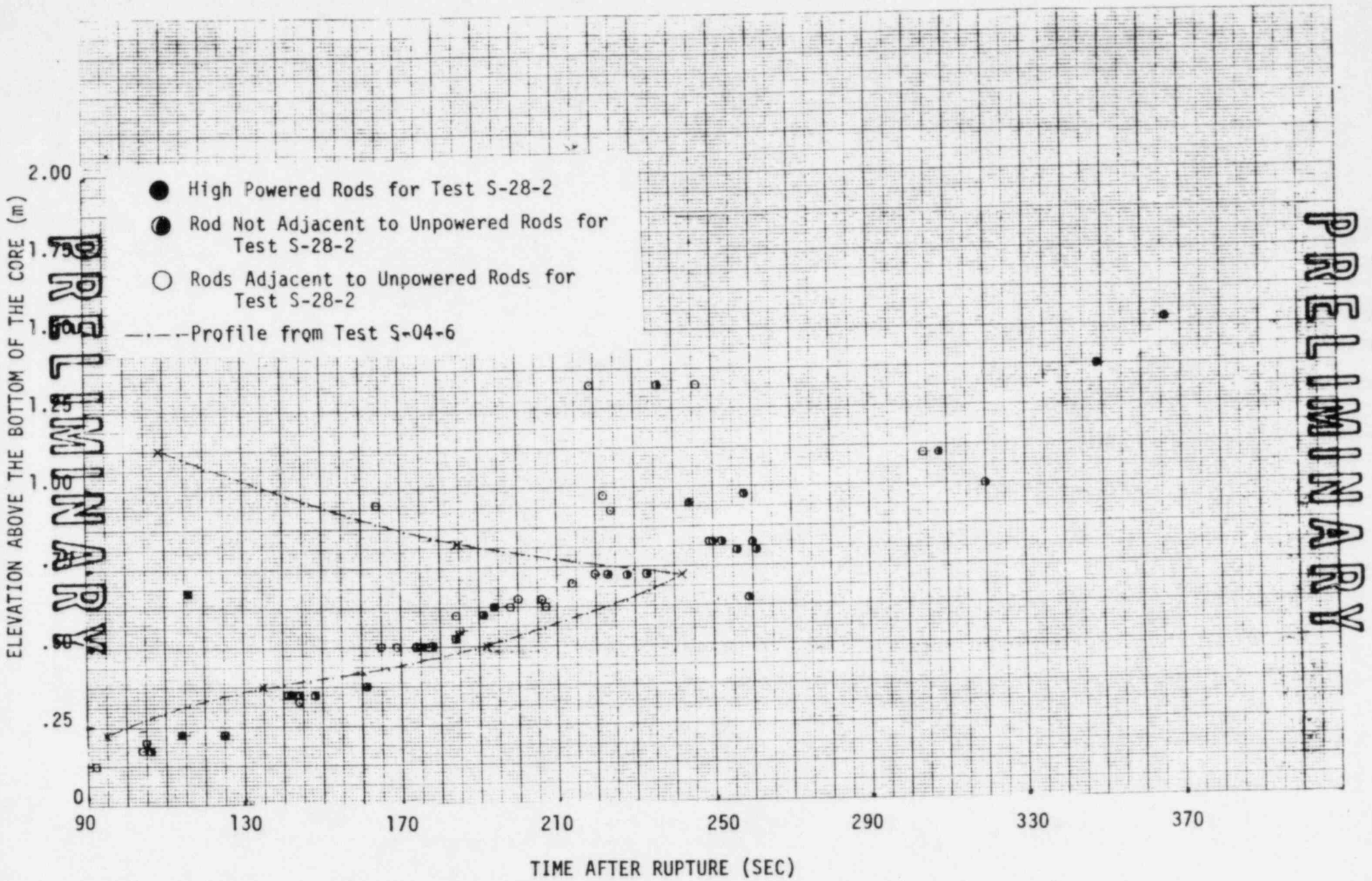

Figure 34. Rod Quench Times Versus Elevation for Test S-28-2

EG&G Idaho, Inc.

P. O. Box 1625
Idaho Falls, Idaho 83401

July 18, 1977

Mr. R. E. Tiller, Director
Reactor Operation and Program Division
Idaho Operations Office - ERDA
Idaho Falls, Idaho 83401

TEST PREDICTION OF SEMISCALE MOD-1 INTEGRAL TEST S-28-5 - DJO-156-77

Reference: D. J. Olson Ltr to P. E. Litteneker, DJO-125-77
Transmittal of Semiscale EOS Appendix 28,
June 3, 1977

Dear Mr. Tiller:

Enclosed is the test prediction document for Test S-28-5 of the steam generator tube rupture test series. Details of the system description and initial test conditions were transmitted in the referenced letter.

The objectives of Test S-28-5 are to aid in defining the core temperature response for large numbers of steam generator tube ruptures and to probe into the range of steam generator tube ruptures shown in the analysis used to specify Test Series 28 to result in high peak cladding temperatures. Test S-28-5 will be a 200% double-ended cold leg break simulation. The rupture of 20 steam generator tubes will be simulated by a flow rate of 0.181 kg/s from accumulator injection into the intact loop hot leg between the pressurizer and the steam generator inlet plenum. The injection will begin at 40 seconds after the initiation of the cold leg break to simulate the steam generator tube ruptures. The change in heat transfer potential of the steam generator will be simulated by discharging the steam generator secondary fluid during the simulated tube rupture period. The system initial conditions and emergency core coolant injection parameters are the same as Test S-04-6, the baseline test for Test Series 28.

The blowdown response should be the same as Test S-04-6 until 40 seconds after rupture. The predictions for the remainder of the transient were performed with the FLOOD4 code. Experimental results from Test S-04-6 indicate the peak rod temperature during blowdown should occur at 8 seconds after rupture when a maximum of 1075 K was achieved. Initiation of the simulated tube ruptures at 40 seconds after rupture should delay the beginning of refill until about 646 seconds after the initiation of the cold leg break and the beginning of reflood until 720 seconds. Both refill and reflood must be accomplished by the high pressure injection

system and the low pressure injection system alone. The peak temperature during reflood was calculated to be 1279 K. The core hot spot is predicted to quench at 846 seconds after rupture and the whole core is expected to quench by 861 seconds. Based on comparisons of past predictions with test data, it is expected that the predicted peak temperatures are higher and the quench times are later than will actually occur during the test.

Very truly yours,

DJ Olson by LGH

D. J. Olson, Manager
Semiscale Program

CPF:emw

Enclosure

cc: R. W. Barber, ERDA
R. S. Brodsky, ERDA
W. W. Bixby, NRC - 2
R. S. Boyd, NRC
S. Fabic, NRC
R. B. Foulds, NRC
R. F. Fraley, ACRS - 21
S. H. Hanauer, NRC
G. Kelly, NRC
S. Levine, NRC
W. C. Lyon, NRC
T. G. McCreless, ACRS
T. E. Murley, NRC
T. M. Novak, NRC
D. F. Ross, NRC
Z. R. Rosztoczy, NRC
R. M. Scroggins, NRC
B. Sheron, NRC
D. E. Solberg, NRC
V. Stello, NRC
R. L. Tedesco, NRC
L. S. Tong, NRC - 2
J. Block, CREARE
G. F. Brockett, ITI
D. M. Chapin, MPR
J. Cudlin, B&W
R. Denning, BCL
G. Fader, CE
G. Farber, IfR
R. Gay, EPRI
P. Griffith, MIT
R. W. Kiehn, EG&G Idaho
W. Kirchner, LASL
M. Levenson, EPRI
W. Loewenstein, EPRI - 2
P. A. Lottes, ANL
J. V. Miller, W
H. P. Pearson, EG&G Idaho - 6
W. Riebold, JRCE
H. Seipel, DBF&T
D. G. Thomas, HNL
D. Trent, PNL
R. J. Beers, ERDA-ID